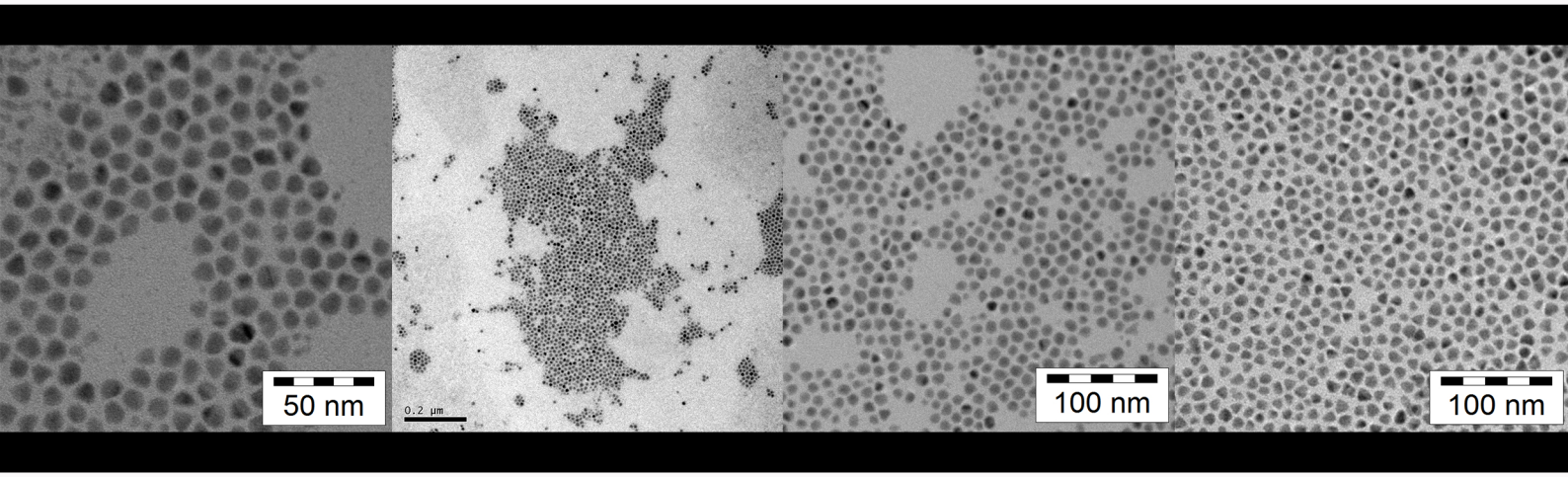

Investigation of PbSe-to-HgSe Cation Exchange & Formation of HgSe Nanocrystals through Digestive Ripening

Master's Research Report
C.D. van Engers

Supervisors:
Dr. M. Casavola
Prof. Dr. D.A.M. Vanmaekelbergh

Condensed Matter and Interfaces
Debye Institute for Nanomaterials Science
Utrecht University
February 2013

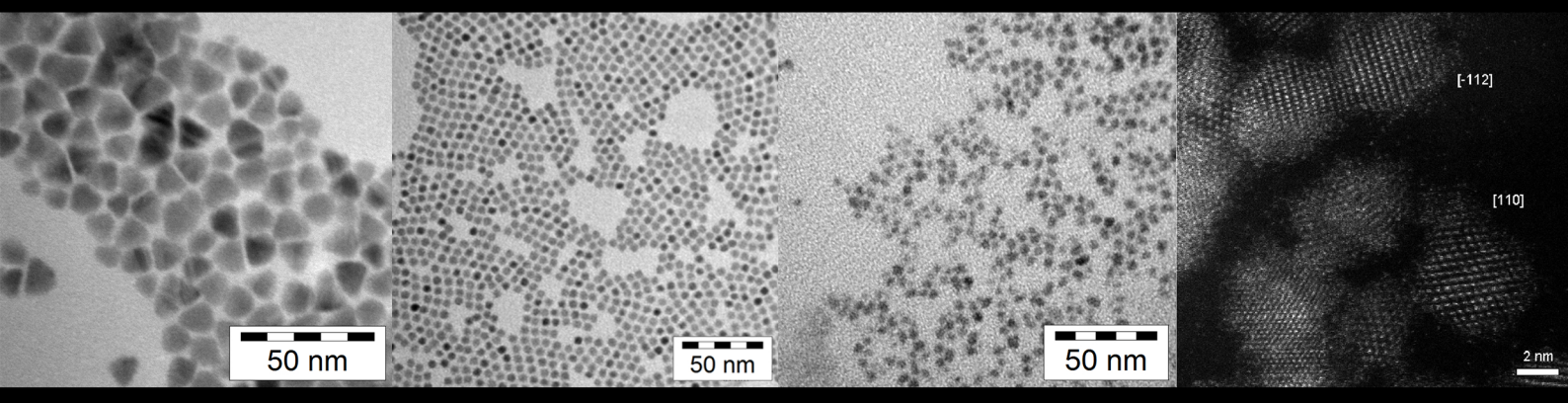

Summary

Ever since their theoretical description in 2005, topological insulators have drawn scientific interest due to their high potential for application in spintronics and quantum computing. In 2007 the existence of this exotic phase of matter was demonstrated experimentally in a HgTe quantum well, fabricated through the use of lithography. Solvo-chemical methods however, are an attractive approach in the synthesis of 0-, 1- and 2-dimensional materials due to their cost-effectiveness. Furthermore solution-processing grants access to a series of facile structural transformations. For example, due to their well-defined geometry, 0-dimensional PbSe quantum dots can be used as building blocks for the formation of 2-dimensional quantum well superlattices through oriented attachment. Subsequently, cation exchange can be used to transform the PbSe quantum well into a selenide of choice. This provides a viable route towards the creation of 2-dimensional compositional analogues that structurally match the topological insulators proposed by theorists.

Therefore, the aim of the project was to investigate the single step cation exchange of PbSe-to-HgSe on both spherical PbSe nanocrystals (NCs) and PbSe quantum wells, since 2-dimensional HgSe superlattices have been proposed to behave as topological insulators. Invested parameters were time, temperature, precursor chemistry, addition of co-ligands, PbSe pre-treatment and cation ratio. The preservation of the anionic framework was not observed. However, HgSe NCs were synthesized through a digestive ripening type reaction. For both PbSe and HgSe, oleic acid was found to serve as solvation framework for the crystal-to-solution phase transitions.

By changing the ratio of Pb and Hg atoms present during the reaction, NCs with an average diameter of about 4 and 9 nm were formed. The 9 nm NCs were found to be HgSe and are formed at a specific (Hg:Pb) ratio. Herein, removal of ligands from the PbSe NCs surface is thought to be an important step needed to be performed prior to Hg-precursor addition. For this purpose thiols (in combination with pyridine) can be used. The 9 nm prism-shaped HgSe NCs are of significantly smaller size dispersion than reported in literature for so far. Furthermore, the synthesis of well-defined, equally shaped crystals is the first step towards their assembly into 2-dimensional superstructures.

Contents

Summary 1

1. Introduction 4

1.1. Everything “nano” 4

1.2. Quantum confinement 4

1.3. A matter of surface control 4

1.4. The driving forces behind cation exchange 5

1.5. The synthesis of mercury selenide nanocrystals 6

1.6. The buildup of this report 7

2. Materials 8

2.1. Chemical 8

2.2. Instrumental 9

3. Experimental 10

3.1. Methods & Results of Precursor Synthesis 10

3.1.1. Synthesis of PbSe Nanocrystals 10

3.1.2. Analysis of PbSe Nanocrystals 11

3.1.3. Synthesis of Hg-precursors 12

3.1.4. Analysis of Hg-precursors 13

3.2. Methods and Results of experiments on *as synthesized* PbSe nanocrystals 14

3.2.1. [3.3 nm PbSe] + [PreHg1] 14

3.2.2. [3.3 nm PbSe] + [PreHgS1,2] 16

3.2.3. [PbSe 5 nm #1] + [PreHg1, 2, 2.2] (+OLAM) 16

3.2.4. Alternative Precursors 22

3.3. PbSe nanocrystals treated with ligand exchange *prior* to Hg-precursor addition 24

3.3.1. [PbSe 5 nm #1](ODT) with [PreHg2.2] 24

3.3.2. Reproducibility: [PbSe 5 nm #2,3](ODT) with [PbHg2.2] 30

4. Discussion 35

4.1. The choice of Hg-precursor and its influence on ion diffusion 35

4.2. Ligand exchange 35

4.3. Oleic acid as solvation framework for solution-to-crystal phase transitions 36

4.4. Ligand exchange using mixed ligands 38

4.5. Comparison to earlier work on HgSe 38

5. Conclusions 40

6. Perspectives 41

6.1. Synthesis optimization 41

6.2. Optical properties 41

6.3. Alternative cation exchange routes 41

7. List of references according to footnotes 42

Appendix A: Supplementary Figures 44
Appendix B: Supplementary Tables 53
Appendix C: List of figures 57
Appendix D: List of Tables 59
Appendix F: Synthesis of CdSe and subsequent cation exchange to Cu_2Se 60

1. Introduction

1.1. Everything "nano"

Nanomaterials are classified by one common denominator; a change in properties that stems from their small dimensions. The changes can be attributed to one (or a combination) of the following:

1. An increase in surface free energy due to an increase in the surface-to-volume ratio.
2. Discretization of the band edges due to a smaller amount of contributing atoms (electrons).
3. Confinement of a physical quantity. [1]

1.2. Quantum confinement

All these qualities are exemplified by the workhorses of the field of semiconductor nanomaterials: lead(II) selenide (PbSe) and cadmium(II) selenide (CdSe)[2]. These nanocrystals (NCs), also referred to as quantum dots (QDs), have been extensively studied for their possible applications as biomedical markers, IR-detectors, solar cells and most recently, in televisions[3] [4]. The main point of interest is their tunable optoelectronic properties, intrinsic to quantum confinement: the spatial confinement of the wavefunction of the exciton.

One of the most striking examples is that of CdSe QDs, for which the band gap can be tuned such that a series of QDs of different sizes luminesces in different colors of the visible spectrum of light (figure 1).

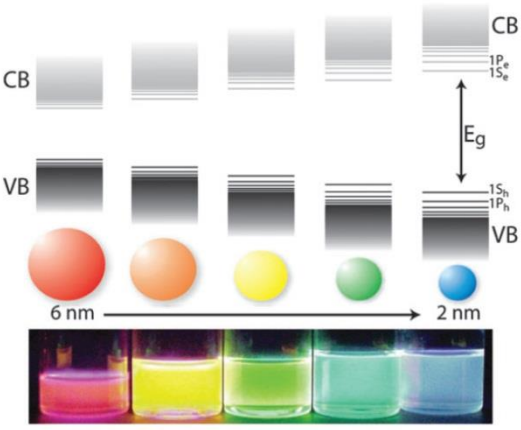

Figure 1. The striking example of quantum confinement in CdSe quantum dots. Figure taken from [1].

1.3. A matter of surface control

The NC-size regime ranges from ~ 1 nm – 100 nm, giving rise to a significant contribution of surface energy to that of the overall system, since a substantial amount of atoms is in close proximity to (and thus strongly influenced by) the surface[5]. As such, solvo-chemical QD-synthesis methods incorporate the passivation of the NC-surface through ligands, similar to organo-metallic interactions in coordination chemistry. In fact, the level of geometric and compositional control that has been achieved can be largely attributed to a juidicious choice of ligands.

A well-known NC-synthesis method is the so-called "hot-injection". The trademark of the hot-injection method is the separation of the nucleation and growth of the NCs. For example, the injection of cold Se-precursor into a hot mixture containing Pb-precursor triggers nucleation and simultaneously induces a drop in temperature. This temperature drop prevents further nucleation, resulting in nearly-monodisperse NCs solutions. Ligands play a multifunctional role during the nucleation stage,

[1] De Mello Donegá, Chem. Soc. Rev. 2011, 40(3), 1512
[2] Hughes et al., ACS Nano 2012, 6, 4573
[3] Talapin et al., Chem. Rev. 2010, 110(1), 389
[4] http://www.nature.com/news/quantum-dots-go-on-display-1.12216 (visited January 29th 2013)
[5] Roduner, Cronin, "Nanoscopic Materials: Size-Dependent Phenomena", Wiley 2006

stabilizing the individual precursors, preformed nuclei, the formed NCs and regulating the diffusion of species present in solution[6]. During the growth stage relative ligand-NC binding energies can be utilized to control the overall morphology resulting in – for example – branched nanocrystals[7]. Next to the manipulation of NC-nucleation and -growth, surface reactivity grants access to new NC structures and compositions through cation exchange or may be used to decrease size dispersion through digestive ripening[8].

Digestive ripening provides a textbook example of how the behavior of nanocrystals, being crystalline "solids", starts to resemble that of molecules. A particularly useful application is the reversible transformation of polydisperse into monodisperse particles as has been reported for Au NCs. For the transformation to monodisperse NCs refluxing for 90 minutes at 110 °C in the presence of excess dodecanethiol is required. The "reverse digestive ripening" requires the removal of DDT and addition of didodecyldimethylammonium bromide[9].

These strongly altered requirements for phase transitions (here: Au moves from the crystal phase, into solution to re-nucleate into the crystal phase again) do not only occur for the strong interaction of Au NCs, MSCs and AuAg or AuCu alloys with thiolates[10] [11] [12] [13]. They have also been observed for Co[14] and PbS[15] NCs.

Cation exchange (CE) entails the replacement of the cations in a NCs and is preferentially performed with preservation of the anion sublattice[16]. Next to using full conversion to unlock materials in novel crystal structures not found in nature, sequential CE grants access to crystals of unique composition unobtainable through any known direct synthesis method[17]. In addition, CE can be combined with direct synthesis in a one pot method where the initial NC-nuclei serve as a template for the target material[18].

1.4. The driving forces behind cation exchange

Cation exchange has successfully been carried out on a variety of NC compositions, finding its theoretical basis within a simple chemical concept: Hard-Soft Acid-Base (HSAB) theory. This theory empirically categorizes Lewis acids and bases on the basis of binding strength to halide ions. Herein hard acids bind in the order $I^- < Br^- < Cl^- < F^-$. Hg^{2+} binds strongly to I^- and is therefore considered as "soft". A useful indicator is the effective electron density of the ion; small cations which are not easily polarizable are hard and form complexes with small anions. Large cations are more polarizable and thus considered soft. A similar classification can be applied to neutral molecular acids and bases[19].

[6] Smith et al., Acc. Chem. Res. 2010, 43 (2), 190
[7] Casavola et al., Nano Lett. 2009, 9 (1), 366
[8] Son et al., Science 2004, 306, 1009
[9] Stoeva et al., Langmuir 2005, 21, 10280
[10] Schaaf et al., J. Phys. Chem. B 1999, 103, 9394
[11] Smetana et al., J. Phys. Chem. B 2006, 110, 2155
[12] Lin et al., J. Nanop. Res. 2002, 2, 157
[13] Rongchao et al., JACS 2004, 126, 9900
[14] Samia et al., JACS 2005, 127, 4126
[15] Hines et al., Adv. Mater. 2003, 15, 1844
[16] Jain et al., JACS 2010, 132, 9997
[17] Miszta et al., ASC Nano 2011, 9, 7176
[18] Kovalenko et al., Angew. Chem. Int. Ed. 2008, 47, 3029
[19] Shriver and Atkins, "Inorganic Chemistry" 4th ed., Oxford University Press

Although HSAB-theory is considered an important concept for CE, ligand-to-metal binding strength[20] and preferential solvation[21] are not the only driving forces for the replacement of one cation by the other. The relative crystal lattice energy of either cation-anion composition and surface free energy both are used as handles in accomplishing these transformations in NC composition[22]. Cation exchange reactions are performed using a variety of conditions ranging from temperatures of 20 °C to 200 °C (as much as the stability of the NCs allows for)[23] to cation ratios of 1 up to 40 or higher[24 25]. The exact mechanism behind cation exchange is not known, but is believed to be associated with formation of vacancies (defects) in the host crystal lattice[26].

1.5. The synthesis of mercury selenide nanocrystals

In 1993 Murray et al. published a reliable synthetic method for preparing CdSe, CdS and CdTe NCs based on organometallic and chalcogenphosphine precursors[27]. From that point on many different methods for metal chalcogenides NC synthesis have been developed creating for example PbSe NCs with quantum efficiencies up to 85% in 2002[28].

For Hg-chalcogenide NCs, luminescent HgTe NCs were first synthesized through a wet chemical synthesis route in the group of Weller in 1999[29]. Efficient emission with a quantum yield of 48% was observed for these spherical QDs. Further work by this group included the synthesis of a very unstable an weak-emitting species of HgSe, for which the luminescence was slightly enhanced by the growth of a CdS shell[30]. Higginson et al. used a similar approach for the synthesis of HgS, however their method resulted in a polydisperse sample with poorly resolved optical transitions compared to the results obtained for CdSe[31].

Hereafter the most significant progress includes the work by Kuno et al., who synthesized HgSe MSCs with a band edge absorption of 595 nm. Smaller clusters could also be synthesized, but no larger NCs were obtained[32]. In fact, most approaches to obtaining larger HgSe NCs result in very polydisperse samples lacking the narrow emission so prized in other members of the metal chalcogenide family.[33 34 35] It is thus clear that, in terms of optical properties and polydispersity, a direct route towards the synthesis of HgSe NCs with efficient luminescence properties (beyond cluster size) has not been shown in literature.

Research interest was renewed in 2005 with the discovery of a new phase of matter, the “topological insulator”. Topological insulators are materials that are insulating in the bulk, but have conducting egde states protected from scattering[36]. Due to the specific electronic structure of HgSe and its strong spin orbit coupling, it is proposed that these edge states exhibit no net conductance, rather a direction

[20] Luther et al., JACS 2009, 131, 16851
[21] Wark et al., JACS 2008, 130, 9950
[22] Rivest et al., Chem. Soc. Rev. 2013, 42, 89
[23] Li et al., Nano Lett. 2011, 11, 4964
[24] Robinson et al., Science 2007, 317, 355
[25] Pietryga et al., JACS 2008, 130 (14), 4879
[26] Casavola et al., Chem. Mat. 2012, 24, 294
[27] Murray et al., JACS 1993, 115, 8705
[28] Wehrenberg et al., J. Phys. Chem. B 2002, 106, 10634
[29] Rogach et al., Adv. Mater. 1999, 11, 552
[30] Harrison et al., Pure Appl. Chem. 2000, 72, 295
[31] Higginson et al., J. Phys. Chem. B 2002, 106, 9982
[32] Kuno et al., J. Phys. Chem. 2003, 107, 5758
[33] Li et al., J. Phys. & Chem. of Sol. 1999, 60, 965
[34] Yang et al., J. Mater. Res. 2002, 17, 1147
[35] Ding et al., Mater. Lett. 2003, 57, 4445
[36] Kane & Moore, *Physicsworld*, February 2011, 32

specific spin current propagates along the surface[37] [38] [39]. Since these surface states are protected from scattering, their potential for spintronics and quantum computing applications is tremendous. Not only is the fundamental size limit of Si-based transistors[40] no longer an issue, different spin states can be used as "bits" (corresponding to either spin-up or spin-down).

Although the topologically insulating state seems a concept out of science fiction, its existence was demonstrated in 2007 for a HgTe quantum well[41]. But the materials composition is not the only parameter of import. A 2-D structure with the periodicity of a honeycomb lattice (similar to graphene) would result in a highly robust topological insulating state (i.e. persistence up to room temperature)[42]. The Vanmaekelbergh-group has already demonstrated that it is possible to form a honeycomb(-like) super-lattice of PbSe QDs through oriented attachment[43]. Therefore combining super-lattice formation with cation exchange provides a promising strategy towards the development of a robust, topologically insulating system.

1.6. The buildup of this report

The goal of this research was the development of a single cation exchange reaction on PbSe QDs to obtain HgSe QDs with preservation of the size and shape. The investigated experimental parameters were time, temperature, precursor chemistry, addition of co-ligands, PbSe pre-treatment and cation ratio. Structural integrity was not retained for the conditions tested (section 3.2). Nevertheless, it was found that PbSe-pretreatment and exposure of the PbSe NCs to specific amounts of Hg-oleate precursor results in the formation of HgSe NCs of low size-dispersion (section 3.3). This behavior is explained on basis of a digestive ripening mechanism (section 4).

[37] Qi et al., Phys. Rev. B 2006, 74, 085308
[38] Qi et al., Physics Today Jan. 2010, 33
[39] Murakami et al., Phys. Rev. Lett. 2004, 93, 156804-1
[40] He and Sun, High-k Gate Dielectrics for CMOS Technology, Wiley 2012, 1st Ed.
[41] König et al., Science 2007, 213, 766
[42] Hasan et al., Rev. Mod. Phys. 2010, 82, 3045
[43] Evers et al., Nano Lett. 2012, ASAP

2. Materials

2.1. Chemical

Table 1. List of Chemicals

Name	Supplier	Abbreviation	Purity	Mol.mass (g/mol)	Density (g/mL)	CAS
Lead(II) acetate trihydrate	Aldrich	$Pb(OAc)_2.H_2O$	99.999%	379.33		6080-56-4
Oleic acid	Aldrich	OLAC	90%	282.46	0.891	112-80-1
1-Octadecene	Aldrich	ODE	90%	170.211	0.789	112-88-9
Selenium powder	Alfa	Se	99.999%	78.96		7782-49-2
Trioctyl phosphine	Aldrich	TOP	90%	370.64	0.831	4731-53-7
Diphenylphosphine	Aldrich	DPP	98%	186.19	1.07	829-85-6
Ethanol, anhydrous	Sial	EtOH	99.8%	46.069	0.8	64-17-5
Buthanol, anhydrous	Sial	BuOH	99.8%	74.1228	0.81	71-36-3
Toluene	Sial	Tol	99.8%	92.1405	0.86	108-88-3
Tetrachloroethylene	Sial	TCE	$\geq$ 99%	165.834	1.62	127-18-4
Isopropanol	Sial	i-PrOH	99.5%	60.0959	0.785	67-63-0
Hexane	Sial	hex	$\geq$ 99%	86.18	0.672	73513-42-5
Mercury(II) acetate	Sial	$Hg(OAc)_2$	99.999%	318.68		1600-27-7
Mercury(II) chloride	Sial	$HgCl_2$	$\geq$ 99.5%	271.5		7487-94-7
Mercury(II) oxide	Sial	HgO	$\geq$ 99.0%	216.59		21908-53-2
Diphenyl ether	Sial	DPE	99%	170.211	1.073	101-84-8
Sodium hydroxide	Sial	NaOH	$\geq$ 97.0%	39.99		1310-73-2
Hydrochloric acid 37%	Mag-Beta	HCl		36.46	0.731	76-47-01-0
Sodium borohydride	Aldrich	$NaBH_4$	98%	37.83		16940-66-2
1-octanethiol	Aldrich	C_8SH	$\geq$ 98.5%	146.29	0.843	111-88-6
Potassium hydroxide	Sial	KOH	$\geq$ 85%	56.11		1310-58-3
Chloroform	Sial	$CHCl_3$	$\geq$ 99%	119.378	1.48	67-66-3
Octylamine	Aldrich	$C_8H_{17}NH_2$	99%	129.24	0.781	111-86-4
Tetrakis(acetronitrile) copper(I)	Aldrich	$[Cu(CH_3CN)_4]PF_6$; tetrakis	No purity given			64443-05-6
Chloroform	Aldrich	Chloroform	99%	119.38	1.483	67-66-3
Oleylamine	Aldrich	OLAM	70%	267.49	0.813	112-90-3
Octadecanethiol	Aldrich	ODT	98%	286.56	0.847	2885-00-9
1-Dodecanethiol	Aldrich	DDT	98%	202.40	0.845	112-55-0
Trioctylphosphine oxide	Aldrich	TOPO	99%	386.63	0.88	78-50-2
Cadmium(II)acetate	Aldrich	$Cd(OAc)_2$	99.99%	266.529		89759-80-8
Ethylene glycol	Aldrich	EG	99.8%	62.07	1.1132	107-21-1

Water (H_2O) was demineralized using a Purite purewater 300.

2.2. Instrumental

General
Due to the toxicity and reactivity of the used materials all experiments were carried out in an inert, nitrogen (N_2) atmosphere, either using Schlenkline techniques or in a N_2-filled glovebox. The cumulative toxicity of Hg-compounds warrants the use of protective clothing and gloves at all times. After precipitation particles were pelleted using a Rotina 38 Hettich Centrifuge operated at speeds between 2500 and 3000 rpm.

Transmission electron microscopy (TEM)
For TEM-measurements, the NCs were diluted and drop-cast onto a copper TEM-grid. Measurements were performed on both a Philips Tecnai 12 and a Philips Tecnai 10 transmission electron microscope operated at 120 kV.

High resolution transition electron microscopy (HR-TEM), Energy dispersive x-ray spectroscopy (EDX) and High angular annular dark field scanning transmission electron microscopy (HAADF-STEM)
The High Angle Annular Dark Field (HAADF)- Scanning Transmission Electron Microscopy (STEM) and STEM-Energy Dispersive X-ray Spectroscopy (STEM-EDX) experiments were carried out by Ke Xiaoxing at EMAT on the HgSe NCs synthesized in initial experiments. The measurements were performed on a FEI Titan 80-300 cubed microscope fitted with an aberration-corrector for the imaging lens and another for the probe forming lens as well as a monochromator, operated at 120kV. The STEM convergence semi-angle used was ~21.4mrad.

Hans Meeldijk from EMU (Electron Microscopy group Utrecht) in Utrecht was responsible for the HR-TEM and EDX-data in later stages of the project. The Images were obtained using a Fei Tecnai20F microscope operated at 200 kV coupled to a Gatan 694 CCD-camera. EDX spectra were recorded using an EDAX-detector.

Scanning Electron Microscopy (SEM)
SEM-EDX spectra were obtained on a Fei XL30SFEG operated at 20 kV. EDX spectra were recorded using an EDAX-detector.

Spectroscopy (Absorption and Emission)
For optical measurements, the NCs were (re)dispersed and diluted in TCE. TCE is the solvent of choice for optical density measurements in the IR, due to its transparency in the IR-region. For absorption measurements, samples were diluted as to have an absorbance between 0.05 and 0.15 for the lowest energy absorption peak. Absorption spectra were measured on a Perkin-Elmer Lambda 950 UV/Vis spectrophotometer.

Emission measurements were carried out at similar dilution as used to obtain the absorption spectra (to prevent any non-linear effects such as self-absorption). The emission spectra were recorded on an Edinburgh Instruments Spectrofluorimeter FLS920 equipped with two detectors for the (near-)infrared region. The R5509-72 detector is sensitive up to 1600 nm; the G5852 detector is sensitive up to 2600 nm. Note that the R5509-72 detector has a higher sensitivity and has to be cooled to -80 °C using liquid nitrogen.

X-ray diffraction (XRD)
For XRD measurements, the NCs were drop cast from solution onto a Si(111) wafer. The liquid was allowed to evaporate leaving a layer of NCs behind. XRD diffractograms were recorded using a setup containing a Philips PW 1729 X-ray generator connected to a Philips PW 1820 diffractometer operated through a Philips PW 3710 mpd control.

3. Experimental

3.1. Methods & Results of Precursor Synthesis

3.1.1. Synthesis of PbSe Nanocrystals

Sample label: [PbSe 3.3 nm], [PbSe 5 nm #1], [PbSe 5 nm #2], [PbSe 5 nm #3]

For the synthesis of PbSe nanocrystals the procedure by Lui et al.[44] was used. Characteristic for this procedure is the utilization of DPP as catalyzing agent for the formation of the PbSe-monomers which later nucleate into PbSe NCs (thought to be the rate limiting step in this "hot injection"-type reaction)[45] [46]. The main advantage of this synthesis, is the large amount of QDs obtained, due to the increased amount of monomers available for the nucleation burst initiated by the injection of TOP-Se into the hot mixture. The disadvantage is the constraints put on the maximal particle size, since a high nucleation burst effectively depletes the monomer reservoir required for further growth (however, this can be tuned by varying DPP-concentration).

Degasing of $Pb(OAc)_2.H_2O$ was performed using a schlenkline setup. The synthesis can be divided into four stages and was carried out as follows:

1. $Pb(OLAC)_2$ precursor preparation

1.897 g ($5*10^{-3}$ mol) ($Pb(OAc)_2.H_2O$) (*white crystals*) was dissolved by heating to 100 °C in 16.0 mL ODE and 3.96 mL ($12.5*10^{-3}$ mol) OLAC in a three-neck roundbottom flask. Subsequently, the mixture is heated to 150 °C under vacuum to remove water and acetate and coordinate the OLAC to the Pb, yielding what is assumed to be the $Pb(OLAC)_2$ precursor in ODE. *The $Pb(OLAC)_2$ precursor is a clear solution.*

2. TOP-Se precursor preparation

Se (*black powder*) and 0.13 mL DPP ($0.75*10^{-3}$ mol) are dissolved in 17.1 mL TOP using mild (80 °C) heating in a small (20 mL) vial and cooled down to room temperature (RT). *The TOP-Se precursor is a clear, slightly yellow solution*.

3. PbSe formation: injection and growth

The $Pb(OLAC)_2$ solution is heated to the injection temperature of 170 °C after which the TOP-Se precursor (RT) is injected into the solution. *Immediately after the injection the solution turns black and the temperature drops to 130 °C.* The mixture is kept at 130 °C for about 30 seconds for growth, after which the reaction is quenched by addition of 20 mL BuOH/EtOH (3:1) and the removal of the heating source.

4. Purification

After quenching, the reaction mixture is allowed to cool to RT. Adding additional EtOH causes *the black solution to become turbid*. The PbSe flocs are pelleted through centrifugation, washed twice by the addition of EtOH and redispersed in toluene.

The abovementioned injection and growth temperatures yield NCs with an average diameter of 3.3 nm. By using an injection temperature of 180 °C and a growth temperature of 150 °C for 5 (or more) minutes, NCs with an average diameter of 5 nm were obtained. The NCs were analyzed using TEM, EDX, Absorption spectroscopy and (in some cases) emission spectroscopy.

[44] Lui et al., Nano lett. 2011, 11, 5349
[45] Steckel et al., JACS 2006, 128, 13032
[46] Evans et al., JACS 2010, 132, 10973

3.1.2. Analysis of PbSe Nanocrystals

An overview of the batches of PbSe nanocrystals with their respective sizes and optical properties is given in table 2. TEM-micrographs are given in figure 2. For ease of reference PbSe NCs of roughly 5 nm in diameter are grouped together as [PbSe 5 nm #1-3]. Spectra are given in supplementary figures S1-4. EDX-analysis performed on PbSe 5 nm #1 showed the (Pb:Se) ratio was (6:4) (supplementary figure S5).

Concentrations were determined using the size-dependent extinction coefficient and related formulas empirically derived by Moreels et al.[47]. Compared to the results found by Moreels et al., there is a discrepancy between the sizes as measured from TEM and those related to the absorption maxima, possibly due to the use of a different synthesis.

Table 2. PbSe Nanocrystal Properties

Batch	Diameter (nm)	Absorption max. (nm)	Emission max. (nm)	(Pb:Se)
PbSe 3.3 nm	3.3 +/- 0.4	1386	1432	
PbSe 5 nm #1	5.0 +/- 0.5	1599	1605	(6:4)
PbSe 5 nm #2	4.9 +/- 0.4	1732		
PbSe 5 nm #3	4.9 +/- 0.4	1724		

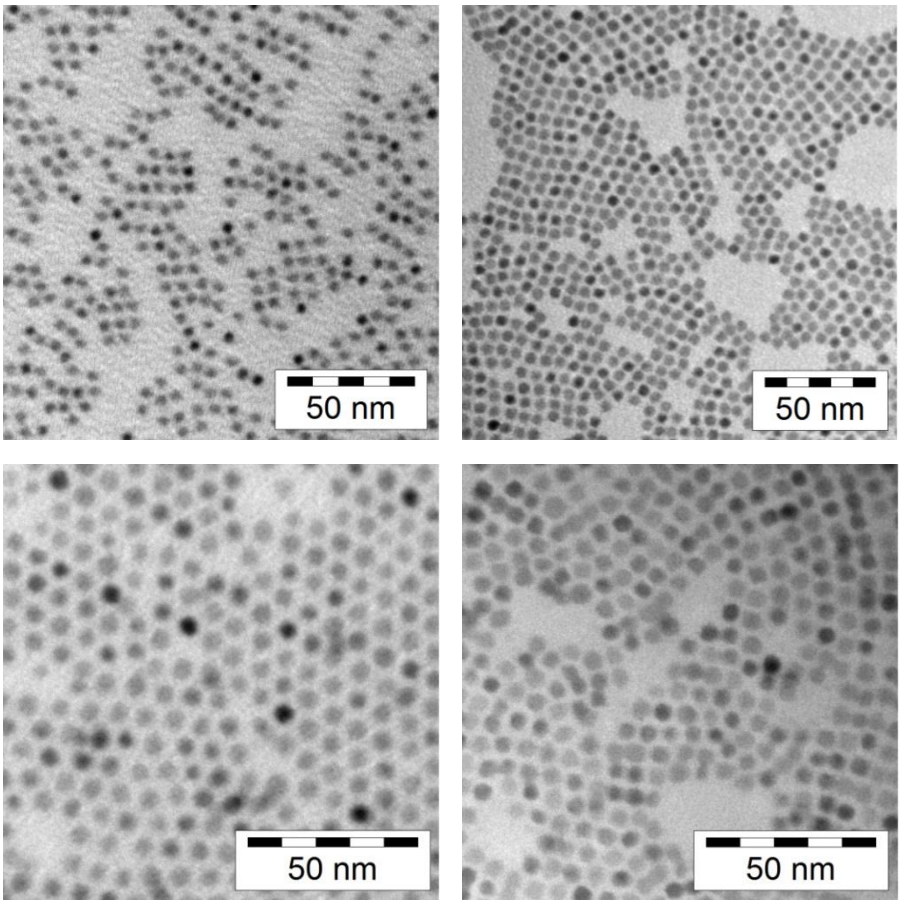

Figure 2. TEM-images of PbSe NCs. Top left: [PbSe 3.3 nm]. Top right: [PbSe 5 nm #1]. Bottom left: [PbSe 5 nm #2]. Bottom right: [PbSe 5 nm #3].

[47] Moreels et al., Chem. Mater. 2007, 19, 6101

3.1.3. Synthesis of Hg-precursors

Mercury oleate ($Hg(OLAC)_2$); [PreHg1], [PreHg2], [PreHg2.2]
This synthesis was adapted from Casavola et al. on the partial CE of CdSe to PbSe/CdSe[48] [49]. The synthesis was performed in a darkened room, since $Hg(OAc)_2$ and other Hg-compounds are sensitive to reduction by light, using a Schlenkline setup. In a typical synthesis $28.4*10^{-3}$ mol OLAC and 22 ml ODE were added to a flask containing $11.7*10^{-3}$ mol $Hg(OAc)_2$. First, the mixture was degased under vacuum at 100 °C for about 1 hour. Second, the mixture was put under N_2 flow and heated to 120 °C for about 2 hours to form the $Hg(OLAC)_2$ complex. *As such, the mixture is transformed from a (slightly yellow depending on OLAC-quality) colorless mixture containing a white solid into a clear yellow liquid.* Finally the mixture was again heated under vacuum for another hour at 100 °C to allow the formed AcOH to escape. In several cases, *a sphere of metallic Hg(l) was formed.* After the mixture was cooled to RT, it was stored in the glovebox.

* If HgO is used instead of $Hg(OAc)_2$ more Hg(l) forms and higher temperatures (up 180 °C) are needed to dissolve the *red solid* and form the $Hg(OLAC)_2$ complex.
** The formation of $Hg(OLAC)_2$ from $HgCl_2$, NaOH and OLAC in H_2O/ODE was shortly investigated, but not optimized as it does not provide a more facile route towards $Hg(OLAC)_2$ synthesis.

Mercury 1-octanethiolates ($Hg(SC_8)_2$ and $Hg(SC_8)Cl$); [PreHgS1,2]
This synthesis was adapted from the work of Smith et al. on the partial CE of CdTe to $Hg_xCd_{1-x}Te$[50]. In a typical synthesis $9.41*10^{-3}$ mol KOH was added to 5 mL MeOH. After dissolution $9.41*10^{-3}$ mol C_8S was added. The *clear solution* was added to a stirred solution of $3.14*10^{-3}$ mol $Hg(OAc)_2$ in 5 mL MeOH. Upto the addition of one molar equivalent of thiolate solution the Hg-solution *becomes a yellow suspension.* In theory this corresponds to the $Hg(SC_8)Cl$ complex; [PreHgS2].
When the added amount of thiolate is increased, *the suspension turns white*. In theory this corresponds to the $Hg(SC_8)_2$ complex [PreHgS1]. After centrifugation the particles were washed thrice with MeOH/$CHCl_3$, dried under vacuum and stored as respectively a *white or yellow powder*.

Mercury oleylamine ($Hg(OLAM)_2$); [PreHg4]
The procedure for the formation of Hg(OLAM) for the direct synthesis of HgTe was used[51]. In a typical synthesis 40 ml (~ $120*10^{-3}$ mol) dried OLAM (*colorless or slightly yellow solution*) was added to 0.275 g ($1*10^{-3}$ mol) $HgCl_2$ (*white crystals*) and heated to 100 °C for 90 minutes. After cooling to RT there is *partial solidification, transforming the clear light yellow solution into a yellow/white suspension.* The mixture was stored under N_2.

Mercurychloride in ethylene glycol ($HgCl_2$/EG); [PreHg5]
For this synthesis, 0.44 g $HgCl_2$ was dissolved in 2.3 mL EG and diluted 10 [PreHg5.1], 100 [PreHg5.2], 1000 times using EG [PreHg5.3].

Mercurychloride in methanol ($HgCl_2$/MeOH); [PreHg6]
For this synthesis 0.136 g $HgCl_2$ was dissolved in 5 mL MeOH to obtain a 0.1 M [Hg^{2+}] solution.

[48] Casavola et al., Chem. Mater. 2012, 24, 294
[49] Pietryga et al., JACS 2008, 130, 4879
[50] Smith et al., JACS 2011, 133, 24
[51] Keuleyan et al., JACS 2011, 133, 16422

3.1.4. Analysis of Hg-precursors

Exact quantification of Hg^{2+}-concentration was not performed. However, due to the nature of the reaction it is assumed that in the final mixture only contains $Hg(OLAC)_2$, free OLAC and ODE. The proposed reaction mechanism is depicted in figure 3: Oleic acid replaces the acetate bound to the Hg after which the acetic acid is evaporated due to its lower boiling point. This effectively drives the equilibrium towards the full conversion into $Hg(OLAC)_2$.

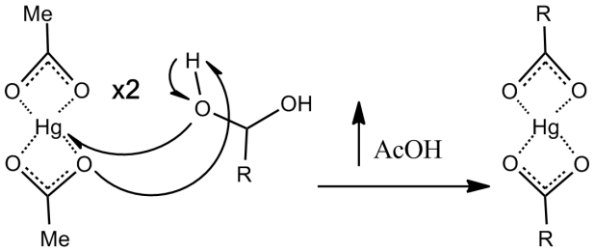

Figure 3. Reaction mechanism of $Hg(OLAC)_2$ formation. R = $-(CH_2)_7HC=CH(CH_2)_7CH_3$. ODE is used as solvent.

The reduction of Hg^{2+} to Hg(l) can only be understood by considering impurities in OLAC (90% pure, section 2.1.) in combination with the elevated temperature and high reduction potential of $Hg^{2+} + 2e^-$ -> Hg[52]. For the determination of the $Hg(OLAC)_2$ concentration it was assumed that the final mixture only contains $Hg(OLAC)_2$, free oleic acid, ODE and metallic Hg(l). Therefore, the final $Hg(OLAC)_2$ concentration was determined by weighing the metallic Hg(l) and subtracting it from the total amount of Hg present at the start of the synthesis. Different concentrations (and ratios) of $[Hg^{2+}]$ in OLAC/ODE were obtained. An overview is given in table 3.

Table 3. $Hg(OLAC)_2$ precursors

Name	$[Hg^{2+}]$ (mol/mL)	$[Hg^{2+}]$:[OLAC]
PreHg1	$5.00*10^{-5}$	1 : 18.9
PreHg2	$19.6*10^{-5}$	1 : 5.10
PreHg2.2	$5.00*10^{-5}$	1 : 18.9

As in other experiments ([PreHgS1, 2] and [PreHg4, 5, 6]) no formation of Hg(l) was observed, the concentration of $[Hg^{2+}]$ was assumed to equal to that of the amount of Hg added.

[52] Physical Chemistry – D.W. Ball, Thomson Learning, Brooks/Cole 2003

3.2. Methods and Results of experiments on *as synthesized* PbSe nanocrystals

This section lists the methods and results of experiments that were performed to verify whether the Pb^{2+}-to-Hg^{2+} cation exchange, from PbSe NCs is feasible or not. As such, Hg^{2+}-precursor was added to the PbSe NCs. All experiments were performed using standard air-free techniques (i.e. in using either Schlenkline or glovebox). In all cases the concentration of [Pb^{2+}] was taken as constant at $4.56*10^{-5}$ M. Thus, for the different sizes PbSe NCs the concentration of particles (and adsorbed ligands etc.) varies.

3.2.1. [3.3 nm PbSe] + [PreHg1]

Pilot experiments [PbHg1]

For the pilot experiments different cation ratios (Hg:Pb = 40, 80) and temperatures (RT, 40°C) were used. An overview is given in table 4. In a (Hg:Pb) = 40 synthesis, two 2 mL aliquots were added to a vial containing a stirred 2,58 mL PbSe solution. The injections were made at t = 0 and t = 30 minutes. Immediately after the first injection, *the black solution became clear, yellow, and then immediately turned black again.* The reaction was quenched after 60 minutes by addition of 5 mL EtOH.

For purification the samples first had to be concentrated by evaporating solvent (under vacuum). Subsequent addition of *i*-PrOH induced flocculation. The samples were washed twice using *i*-PrOH/Tol and analyzed with TEM. HAADF-STEM and EDX measurements on sample [PbHg1_3] were performed at EMAT (University of Antwerp). The results are shown in figure 4. Optical measurements were performed, showing the disappearance of excitonic features in the absorption spectrum accompanied with broad, weak emission (supplementary figures S6, S7).

Table 4. Experimental conditions and results of pilot experiments

Name	(Hg:Pb)	Temperature (°C)	Size (nm)
PbHg1_1	**40**	RT	3.1 +/- 0.5
PbHg1_3	**40**	50°C	3.8 +/- 0.6
PbHg1_4	**80**	50°C	3.9 +/- 0.5

Comparing the TEM-images of the original [PbSe 3.3 nm] (figure 2) and the NCs after the reaction (figure 4A-C), that the shape and size have not been retained. Furthermore, EDX (figure 4F) evidences the presence of Hg, but not of Pb. Clearly, HgSe has been formed, but not by a standard CE reaction. Rather, the (anion sub-)lattice has been distorted. If the formation of HgSe is considered to be favored, then a high exchange ratio would provide a very strong driving force that may induce shape changes during a very violent exchange reaction. Therefor “milder” conditions were chosen.

Post-pilot experiments [PbHg2]

Post-pilot experiments on [PbSe 3.3 nm] NCs were performed at RT and -10 °C, using lower exchange ratio of 5. Only 1 Hg-precursor injection was made at t = 0, and the reaction was quenched after 30 minutes, again by addition of anti-solvent. TEM-analysis on both samples clearly shows both size and shape were not retained (table 5)(supplementary figures S8, S9) compared to the original [PbSe 3.3 nm] (figure 4).

Note that again the addition of anti-solvent was insufficient to induce flocculation and that the same extended (vacuum) work-up procedure was required. Further, it is debatable whether the reaction is actually quenched upon anti-solvent addition, since no (phase-) separation of NCs from the reaction mixture takes place.

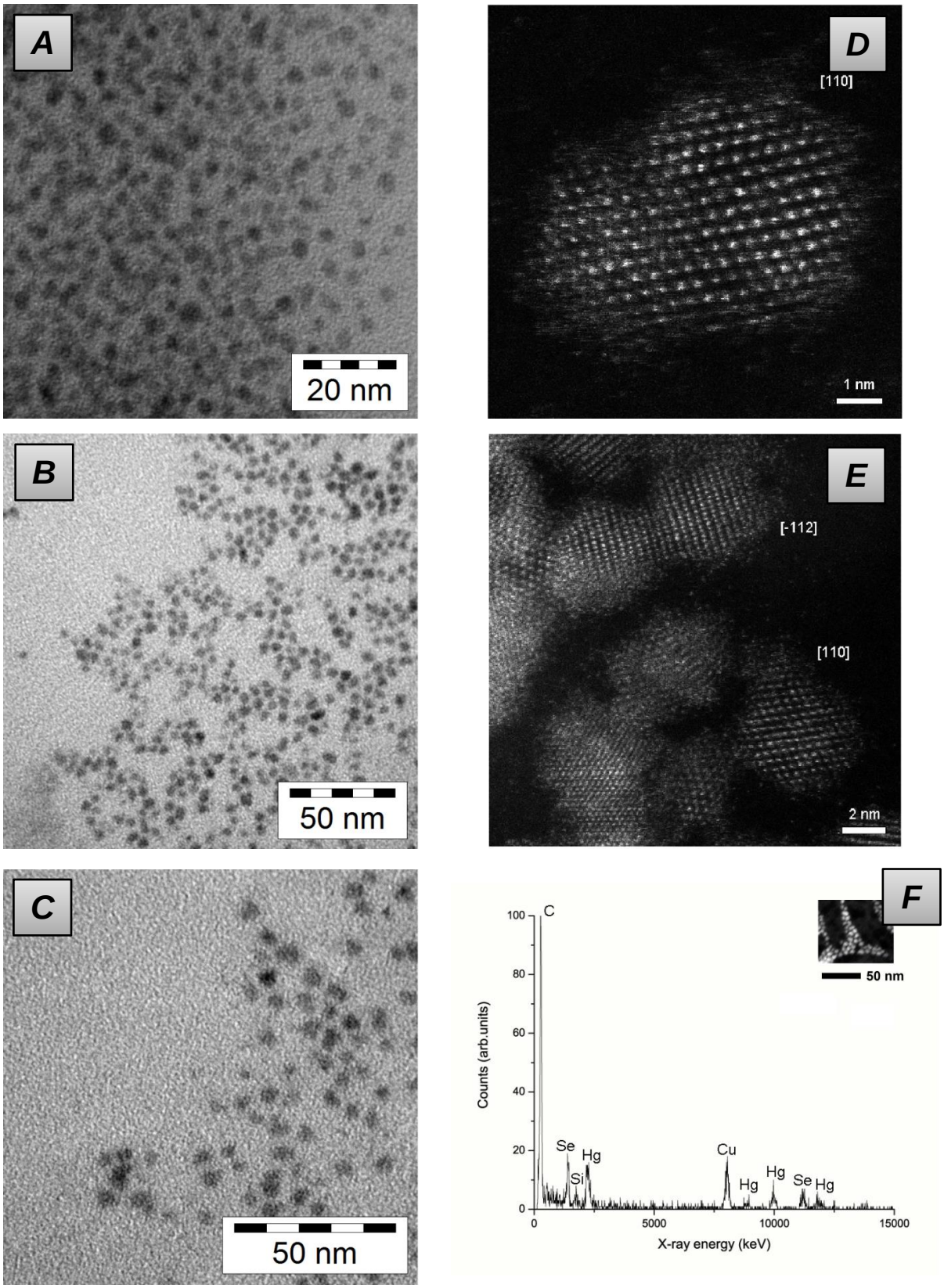

Figure 4. Results of pilot experiments. A;B;C) TEM images of [PbHg1_1], [PbHg1_3], [PbHg1_4] resp.; D;E) HAADF-STEM images of [PbHg1_3]; F) EDX-spectrum of [PbHg1_3].

Table 5. Experimental conditions and results for [PbHg2_RT] & [PbHg2_-10]

Name	(Hg:Pb)	Temperature (°C)	Size (nm)
PbHg2_RT	**5**	RT	3.8 +/- 0.6 nm
PbHg2_-10	**5**	-10	2.6 +/- 0.5 nm 10.3 +/- 1.0 nm

3.2.2. [3.3 nm PbSe] + [PreHgS1,2]

[PbHg2S]

As alternative to the $Hg(OLAC)_2$ precursor, [PreHg1], several reactions were performed using [PreHgS1,2]. The use of mercury 1-octanethiolates was inspired by the results of Smith et al.[53] who successfully utilized the $Hg(SC_8)_2$ compound to convert CdTe into $Hg_xCd_{1-x}Te$. The synthesis was carried out in a similar manner to the [PbHg2]-series, yielding a monodisperse sample of spherical NCs. However, SEM-EDX revealed the particles to be PbSe (see figures S10, S11, and table S1 of supplementary information).

3.2.3. [PbSe 5 nm #1] + [PreHg1, 2, 2.2] (+OLAM)

From the experiments on [PbSe 3.3 nm] it was clear that neither size nor shape were preserved. Previous work by Son et al.[54] on the CdSe/AgSe CE system indicated that below a critical NC size (~ 4 nm), shape and size are no longer preserved. Therefor the choice to switch to a larger (5 nm PbSe) system was made.

[PbHg3] and [PbHg3.2]

The first experiments on [PbSe 5 nm #1] were performed in similar manner to [PbHg2], (i.e. Hg-precursor injection to a stirred solution of PbSe NCs). All experiments were performed at room temperature (glovebox temperature, 25 – 30 °C). TEM-images of the analyzed samples show either anisotropic particles that have been reduced in size or, in a few cases, larger particles with prism-like shape (in a 2-D projection: TEM-image). Table 6 lists the corresponding conditions used. Figure 5 shows a typical TEM image of both the triangles (A), as well as the anisotropic NCs (B). For some samples a mixture of both was found. Remarkably in both cases shape and size deviate from that of the original spherical 5 nm PbSe NCs (figure 2). The image most likely represents HgSe NCs, which have a zinc blende (ZB) structure in the bulk and is its thermodynamically most stable structure [5556]. Futhermore, from EDX associated with HR-TEM we have found prims-shaped particles to be compatible with HgSe (section 3.3)

[53] Smith et al., JACS 2011, 133, 24
[54] Son et al., Science 2004, 306, 1009
[55] Wolfe, “Physical Properties of Semiconductors”, Prentence Hall ,New York, 1989
[56] Jayaraman et al., Phys. Rev. 1963, 130, 2277

Table 6. [PbHg3], [PbHg3.2] conditions and results

Name	(Hg:Pb)	Reaction time (min)	Size (nm)
PbHg3_1	5	30	4.6 +/- 0.6
PbHg3_2	1	30	7.0 +/- 0.9 3.5 +/- 0.5
PbHg3_3	5	1	3.9 +/- 0.6
PbHg3_4	1	1	8.9 +/- 1.7
PbHg3.2_1	5	30	3.9 +/- 0.5
PbHg3.2_2	1	30	6.7 +/- 0.8 *(few)* 3.4 +/- 0.5
PbHg3.2_3	5	1	3.1 +/- 0.8
PbHg3.2_4	1	1	7.5 +/- 1.1 *(few)* 3.1 +/- 0.4

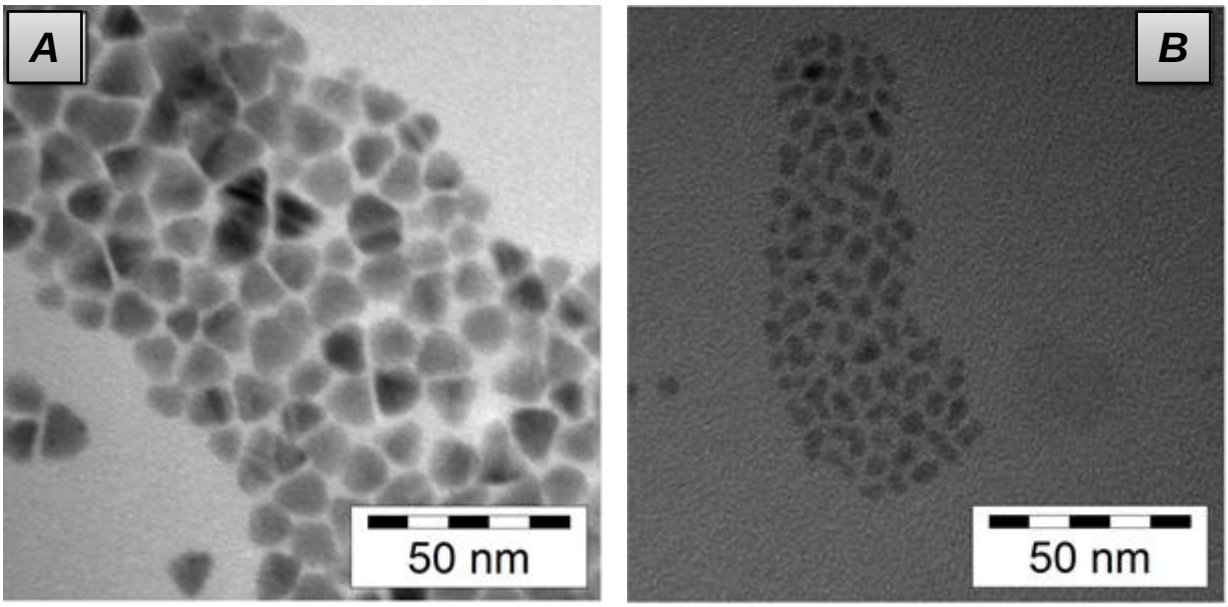

Figure 5. TEM images of A) (2D)-triangular NCs, (actual sample: [PbHg3_4]); B) Anisotropic NCs (actual sample [PbHg4_1]).

Changing from [PbHg1] to [PbHg2]

For the next series of experiments a different $Hg(OLAC)_2$-precursor was used:

For [PbHg3] and [PbHg3.2] Hg-precursor [PreHg1] was used. Due to depletion of this precursor, [PreHg2] was synthesized. It is known that during the synthesis of this precursor, less Hg(l) was formed (table 3, section 3.1.4.). Therefor the concentration of Hg^{2+}-ions in solution was higher than for [PreHg1]. At the same time, the effective concentration of free $OLAC^-$ in these experiments is lower.

This difference in $[Hg^{2+}]$:$[OLAC^-]$ induced aggregation of NCs in many of the experiments, therefor OLAM was introduced as co-solvent/ligand in the [PbHg4N]-series. Finally, a mixture of OLAC in ODE was added to [PreHg2] to obtain a precursor that is presumed to be similar to [PreHg1] in terms of $[Hg^{2+}]$ and $[OLAC^-]$. This Hg-precursor is referred to as [PreHg2.2].

[PbHg3.3], [PbHg4N] (using [PreHg2]), [PbHg7, 7.2] (using [PreHg2.2])

The formation of triangular HgSe NCs of the quality shown in figure 5A has not been shown in literature. In fact, luminescence from HgSe NCs in this size regime (> 3 nm, see section 4.5) would be unique. Therefore efforts were made to either reproduce the results of [PbHg3_2] and [PbHg3_4], in

which the HgSe triangles were the dominant species in the sample or obtain a sample in which both size and shape of the crystals had been preserved.

Experimental series [PbHg3.3] and [PbHg7, 7.2] were performed with the goal of reproducing the formed triangles. Special focus was put on heating the sample, since the [PbHg3] samples were heated to ~ 80 °C to increase the speed of solvent evaporation in the first purification step. For [PbHg3.3], [PbHg2] was used as precursor. The Hg-precursor for [PbHg7, 7.2] was [PbHg2.2].

Since the experiments performed using [PreHg2], often induced (irreversible) aggregation, - and to test the effect of adding a co-ligand – a series of experiments was performed where the influence of the presence of OLAM was tested: [PbHg4N] was performed with and without added OLAM of a volume equivalent to that of the reaction mixture. OLAM was added before addition of the Hg-precursor. Since the mixture is a diluted suspension of NCs, the additional OLAM is present is large excess compared to ligands on the surface of the NCs.

A typical TEM-image of the obtained results is shown in figure 6. Comparing the results to TEM-images of the original [PbSe 5 nm #1] particles (figure 2), it is clear that size nor shape are preserved. Further, no sample containing “triangles” was observed**.** The only real difference between using either [PreHg2.2], [PreHg2] + OLAM or [PreHg2] is the extent aggregation of particles at higher temperature. An overview of tested conditions and results can be found in supplementary tables S3-5.

The results clearly indicated that even in conditions such as room temperature, low cation ratio and an excess of ligands present in solution, structural integrity was not maintained.

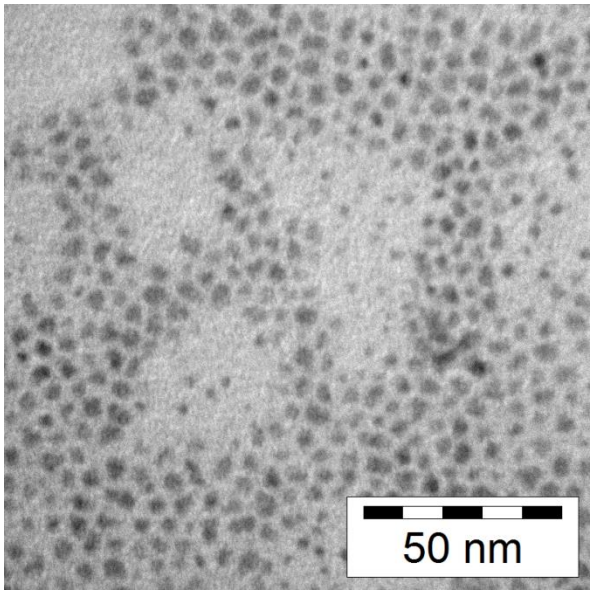

Figure 6. TEM-image of a typical [PbHg3.3], [PbHg4N] or [PbHg7, 7.2] result (original sample: [PbHg4N_G]).

[PbHg5] (using [PreHg2.2])

To investigate the evolution of the reaction mixture from the first moments of Hg-precursor addition, an experiment was performed where samples were drop cast directly from solution onto a TEM-grid during the course of the reaction. An added benefit to this approach is the fact there lies no uncertainty in the effect of adding a “quenching” antisolvent (as mentioned in 3.2.1.). Note that from this point on [PreHg2.2] was used as Hg-precursor. The results of the first samples taken are shown in figure 7 and table 7**.** Note that after the first two sampling, the amount of injected precursor was gradually increased. For these conditions samples were also taken, but are omitted for clarity. The data can be found in supplementary table S7.

Table 7. Results and conditions of first samples taken from [PbHg5]

Name	(Hg:Pb)	Reaction time (s)	Temperature (°C)	Size (nm)
PbHg5_A	1	15	RT	4.0 +/- 1.1
PbHg5_B	1	30	RT	Between 3 - 10
PbHg5_E	1	15	50	4.2 +/- 0.8
PbHg5_F	1	30	50	3.4 +/- 0.7
PbHg5_EH	13.2	300	50	3.5 +/- 0.4

Upon examination of the TEM-images in figure 7A and 7B compared to an image of the original particles (figure 7F) it is very clear that even at mild conditions the structural integrity of the PbSe NCs is broken immediately after the addition of $Hg(OLAC)_2$. The NCs do seem to eventually evolve to an equilibrium shape (figure 7C, D), but are still markedly polydisperse and anisotropic.

Since [PbHg5_EH] does show some decrease in polydispersity, EDX was performed to determine the elemental composition. However the data obtained indicate that the final product contains a mix of Pb and Hg of about 15 % and 35 % respectively (complementary figures S16, S19, S20). This result seems contradictory to what would be expected considering the results obtained for [PbHg1], which showed particles of similar shape and size, being composed of pure HgSe, when a ratio of (Hg:Pb) = 40 was used.

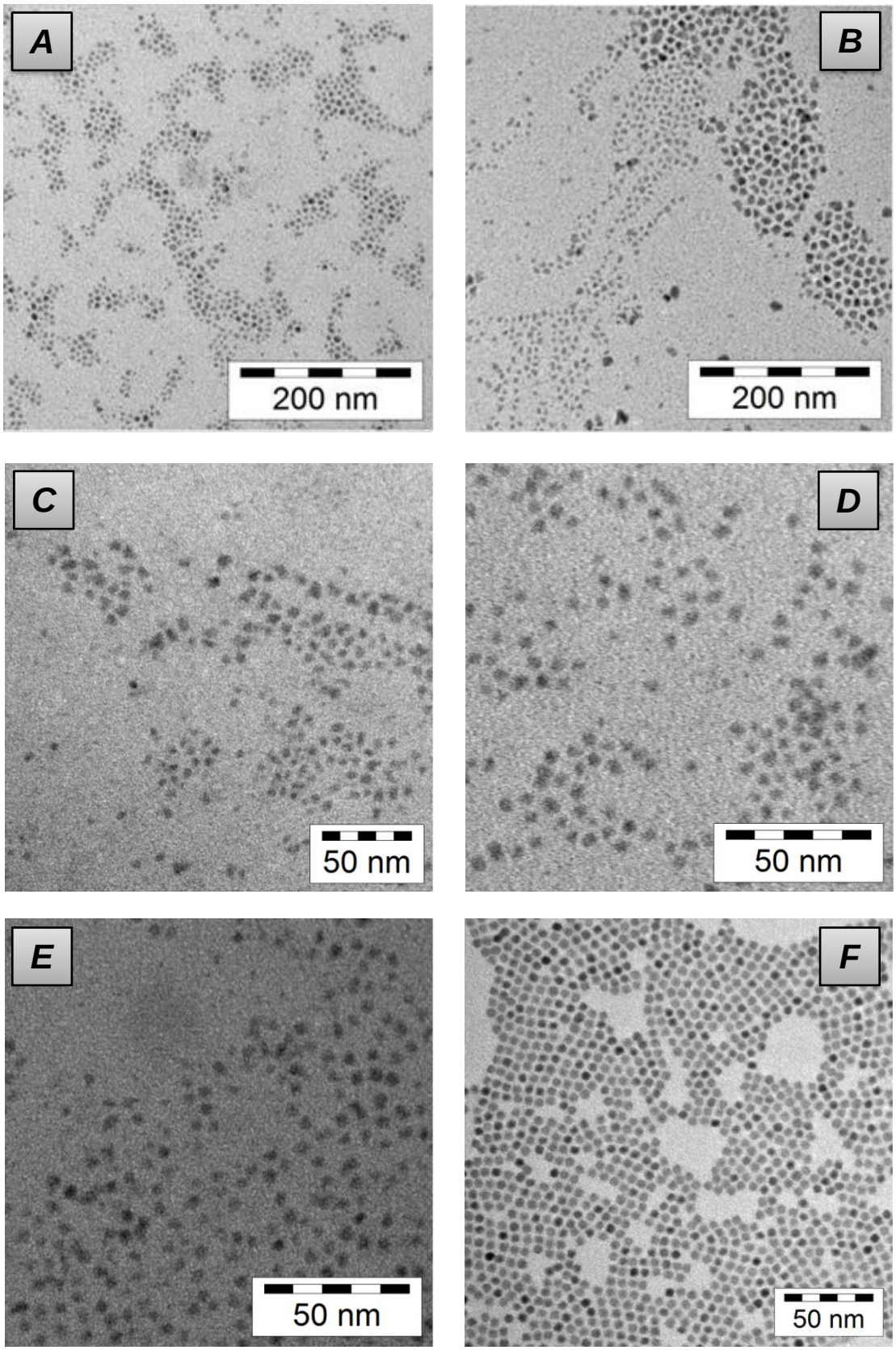

Figure 7. TEM-images of the temporal evolution of NCs in solution: A) [PbHg5_A]; B) [PbHg5_B]; C) [PbHg5_E]; D) [PbHg5_F]; E) [PbHg5_EH]; F) [PbSe 5 nm #1]

[PbHg5.2], [PbHg5.3]
Several control experiments were performed to validate the results obtained for [PbHg5_EH]. SEM- and TEM-EDX measurements confirmed that there was no complete conversion from Pb-to-Hg. Both an overview of results and conditions, and the spectra are provided in the supplementary table S7 and figures S17, S18. All data so far points to a very reactive system evolving to a preferred state (with a certain spread of sizes and shapes).

[PbHgSheet]
In a second step, the cation exchange on PbSe superlattices instead of self-standing colloidal QDs was attempted. The conversion of PbSe nanosheets into HgSe would be of great interest in the fabrication of 2-dimensional nanomaterials with topologically insulating behavior. Compared to the colloidal 0-dimensional NPs that have a large surface-to-volume ratio, PbSe nanosheets represent a more rigid structure and are expected to retain their geometry under cation exchange conditions. Therefore, different behavior was expected.

The super-lattice was prepared by drop-casting a solution of PbSe NCs (provided by W.H. Evers) in toluene on ethylene glycol (EG) according to the procedure by Evers et al.[57]. After the toluene evaporates, the super-lattice is scooped up from the EG by a carbon coated copper TEM-grid and placed under vacuum to evaporate EG left on the grid. After drying for ~ 1 hour, the grid was analyzed by TEM. The resulting super-lattice, analyzed by TEM, consists of a network of oriented attached PbSe NCs (figure 8).

Multiple grids can be scooped from the same sample. Therefor another grid was used to scoop and subsequently dip the material in a solution containing the $Hg(OLAC)_2$ precursor. After exposure to Hg-precursor for about 30 seconds, the sample was washed by dipping it in BuOH/MeOH /toluene thrice. The sample was analyzed with TEM (figure 8) and SEM-EDX. SEM-EDX revealed the super-lattice to be pure PbSe (supplementary figure S21, S22).

Comparing the TEM-images in figure 8, it is clear that the individual “network branches” have been reduced in size. Taking into account the information obtained from EDX, one reaches a striking conclusion: the PbSe surface seems to be etched through the presence of $Hg(OLAC)_2$. Considering earlier results obtained for the cation exchange on the free-standing PbSe QDs, it is concluded that the change in shape results from particle dissolution and re-nucleation.

[57] Evers et al., Nano Lett. 2012, ASAP

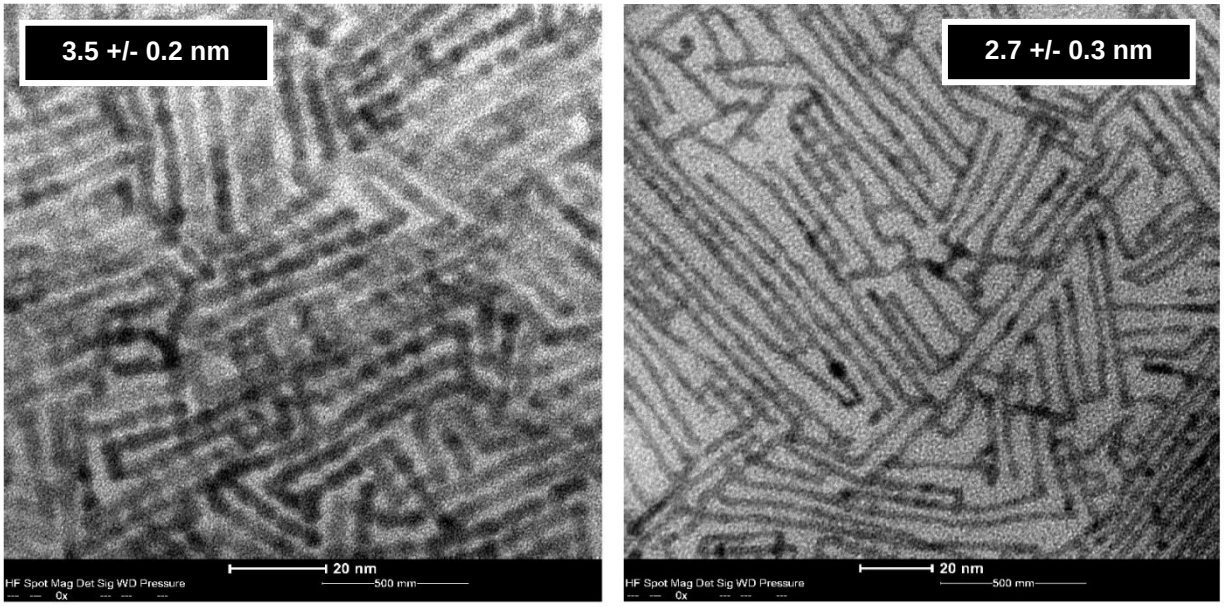

Figure 8. TEM-images of PbSe NCs super-lattices. Left, before addition of Hg-precursor – average diameter 3.5 +/- 0.2 nm; right, after Hg-precursor addition – average diameter 2.7 +/- 0.3 nm.

3.2.4. Alternative Precursors

The effect of alternative precursors was also investigated. This essay mainly serves to test the correctness of the initial assumption made when choosing the use of $Hg(OLAC)_2$ on the basis of the HSAB-theory. Hg and Cd have smaller a cationic radius than Pb[58]. As a result, Pb can be regarded as a "softer" acid than Hg and Cd. According to HSAB-theory, ligand-affinity can provide a thermodynamic driving force if the ligands presenting Hg^{2+} (the ligands in solution) bind more strongly to Pb^{2+} (section 1.5).

[PbHg3S], [PbHg8,8.2], [PbHg5.3_C1, C2]
The experiments were performed analogues to the earlier synthesis; Hg-precursor was added to a stirred solution of [PbSe 5 nm #1] NCs. In the case of [PbHg5.3_C1, C2], small aliquots of ODT (Volume $Hg(OLAC)_2$:ODT = 80) were added immediately after the addition of $Hg(OLAC)_2$. For [PbHg3S], [PreHgS1] was used and for [PbHg8,8.2], [PreHg4] was used.

The results were initially analyzed with TEM, showings both size and shape had been retained. However, EDX analysis revealed the particles to be PbSe. TEM-images and EDX-spectra can be found in supplementary figures S12-15 and supplementary tables S2, S7, S8.

These results indicate that initial choice for $Hg(OLAC)_2$ as Hg-precursor was better in terms of HSAB-theory; using thiolate or amine-type precursors results in neither exchange nor etching, indicating that the Hg-precursor is stable in solution and that the Pb^{2+} cations are stable in the crystal phase.

[PbHg6,6.2]
[PreHg5] was used in a method similar to the one described for the formations of PbSe NC super-lattices, instead of ethylene glycol. Even though the particles were thoroughly washed, the resulting TEM-images were hard to resolve, showing polydisperse particles with anisotropic shapes. The use of [PreHg5] was not investigated any further. Results can be found in supplementary table S8.

[58] R.D. Shannon, Acta Cryst. 1976, A 32, 751

[PreHg6] + [PbSe 5 nm #1]

The addition of $HgCl_2$ in MeOH to [PbSe 5 nm #1] was shortly investigated. Addition of the Hg-precursor resulted in the immediate formation of a *insoluble white solid in a clear colorless solution.* The reaction was not investigated any further.

3.3. PbSe nanocrystals treated with ligand exchange *prior* to Hg-precursor addition

As the experiments on [PbHgSheet] showed dissolution and – in the case of the PbSe NCs – re-deposition/re-nucleation occur during the reaction, the stabilization of the NCs through surface modification was attempted. This approach was motivated by the work of Wang et al.[59], who observed that when a thiol,(DDT) was introduced during cation exchange from CdTe-to-$Hg_xCd_{1-x}Te$, a Hg-thiolate complex formed at the surface of the NCs.

Wang et al. claim that this complex acts as mediator during cation exchange, as the resulting particles maintain their high luminescence QY. A high QY indicates that the non-radiative decay component is small, which is commonly associated with a small number of surface traps. As such it is assumed that the authors are dealing with either one or both possible situations:

1. The surface Hg-complex indeed acts as mediator, facilitating the introduction of Hg^{2+} and dissociation of Pb^{2+} ions from the NC.
2. The surface Hg-complex forms a protective layer, passivating surface traps in a similar fashion to $Pb(OLAC)^+$ for PbSe[60].

The main difference compared to the PbSe NCs, is that Hg-thiolates form a polymeric seperate phase, thus during XRD-analysis sharp peaks corresponding to this complex may be found[61] [62] [63]. Even though addition of ODT during the reaction yielded no results ([PbHg5.3_C1, C2]), the alternative situation of having ODT at the NC-surface prior to the reaction was investigated.

The introduction of ODT during the first step of NC purification, was found to be critical for maintaining colloidal stability in the direct synthesis of HgTe by Keuleyan et al.[64]. Therefor ODT was chosen over DDT.

3.3.1. [PbSe 5 nm #1](ODT) with [PreHg2.2]

Ligand exchange was performed on several batches of the 5 nm PbSe QDs. In order to achieve complete conversion, an equivalent volume of ligands was added to a stirred suspension of the 5 nm PbSe QDs under slight heating. Since the QDs are suspended in toluene with ligands on the surface, the addition of an equivalent volume of to-be-exchanged ligands is assumed to be in large excess; enough to drive the solvent-ligand equilibrium towards a full ligand exchange. As such, ligand exchange was presumed to be successful (although, ideally quantitative analysis using (FT)-IR spectroscopy should be performed).

The temperature of the heating plate was set to 45 °C and the samples were left for 48+ hours. After this period, the QDs were precipitated by addition of BuOH/MeOH (3:1), pelleted by centrifugation, re-suspended in toluene and washed once using BuOH/MeOH (1:1) and once using MeOH. *After addition of ODT the PbSe suspension turns turbid and remains so after purification*. Neither polar nor apolar solvent is able to completely redisperse the particles.

When scattering was not the dominant contribution to the signal (due to the fact the samples were turbid), PLS-measurements were used to determine the concentration. Otherwise, the QD-

[59] Wang et al., Dalton Tran. 2012, 41, 12726
[60] Lingley et al., Nano Lett. 2011, 11, 2887
[61] Hoffmann et al., Inorg. Chem. 2001, 40, 977
[62] Canty et al., Inorg. Chim. Acta 1977, 24, 109
[63] Bochmann et al., J. Chem. Soc. Dalt. Trans. 1991, 2325
[64] Keuleyan et al., JACS 2011, 133, 16422

concentration was assumed to resemble the pre-exchange value, since no material is lost (and the starting volumes and concentrations are known).

[PbHg9, 9.2, 9.3]

The experiments were performed in a manner similar to earlier experiments, using the same Pb^{2+} concentration and [HgPre2.2] as Hg-precursor. The results are given in table 8 and figure 9**.**

Table 8. Conditions and results of [PbHg9]

Name	T (°C)	t (min)	(Hg:Pb)	Size (nm)	Shape	Description
PbHg9_A	RT	0.5	1	3.9 +/- 0.8	Anisotropic	Larger species present?
PbHg9_B	RT	5	13.2	~ 3.2	Anisotropic	Very blurry (dirty) TEM-photo
PbHg9_C	50	0.5	1	6.5 +/- 0.9 3.8 +/- 0.5	Anisotropic	Large triangles and smaller spheres?

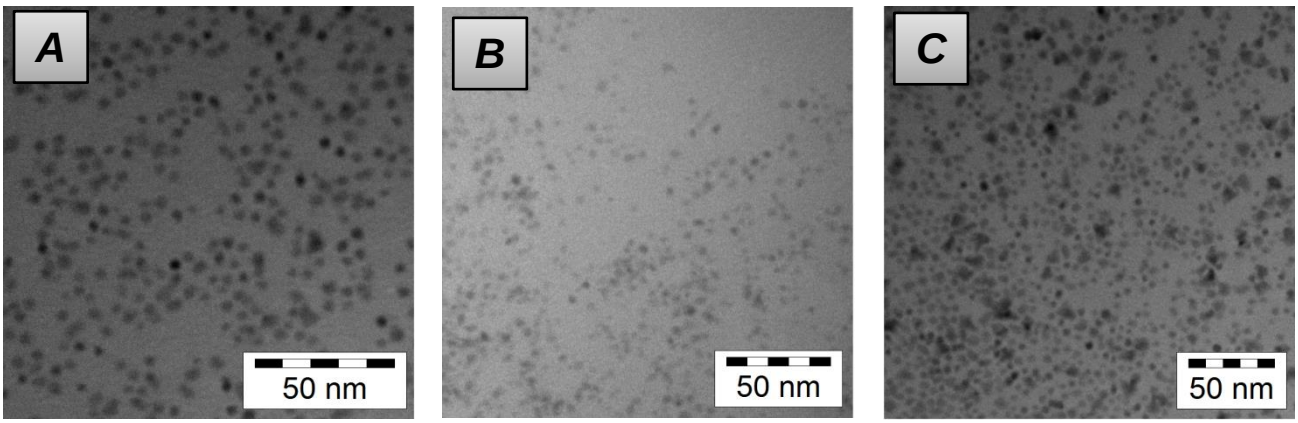

Figure 9. TEM-images of [PbHg9], the image labels correspond to X = A,B,C, respectively

Figure 9 C shows the appearance of triangular shaped particles (as 2D-TEM projection). Motivated by their appearance, the temporal evolution of the crystals at 50 °C and 80 °C was investigated further, by dropcasting samples directly on a TEM-grid during the course of the reaction. The results are given in table 9 and figure 10**.** Note that at temperatures of 80 °C and higher, and equivalent volume of ODE was added to the PbSe QD suspension to ensure solution stability at higher temperature.

Table 9. Results and conditions of [PbHg9.2]

Name	T (°C)	t (min)	(Hg:Pb)	Size (nm)	Shape	Description
PbHg9.2_50_5	50	5	1	4.6 +/- 0.9	Spherical	very polydisperse, many different sizes, also different shapes present
PbHg9.2_50_10	50	10	1	6.7 +/- 1.0 4.2 +/- 0.7	Large anisotropic + small spherical	
PbHg9.2_50_15	50	15	1	7.8 +/- 1.3 4.1 +/- 0.7	Large angular + small spherical	
PbHg9.2_50_30	50	30	1	8.9 +/- 1.2 4.4 +/- 0.8	Large anisotropic + smaller spherical	
PbHg9.2_50_60	50	60	1	13.8 +/- 2.4	Large triangles + background of small material	
PbHg9.2_80_5	80	5	1	8.1 +/- 1.1	Predominantly Triangular	
PbHg9.2_80_10	80	10	1	9.4 +/- 1.2 ~ 2.5	Predominantly triangular	
PbHg9.2_80_15	80	15	1	9.2 +/- 1.2	Triangular	
PbHg9.2_80_30	80	30	1	9.8 +/- 1.2	Triangular	
PbHg9.2_80_60	80	60	1	10.3 +/- 0.9	Triangular	

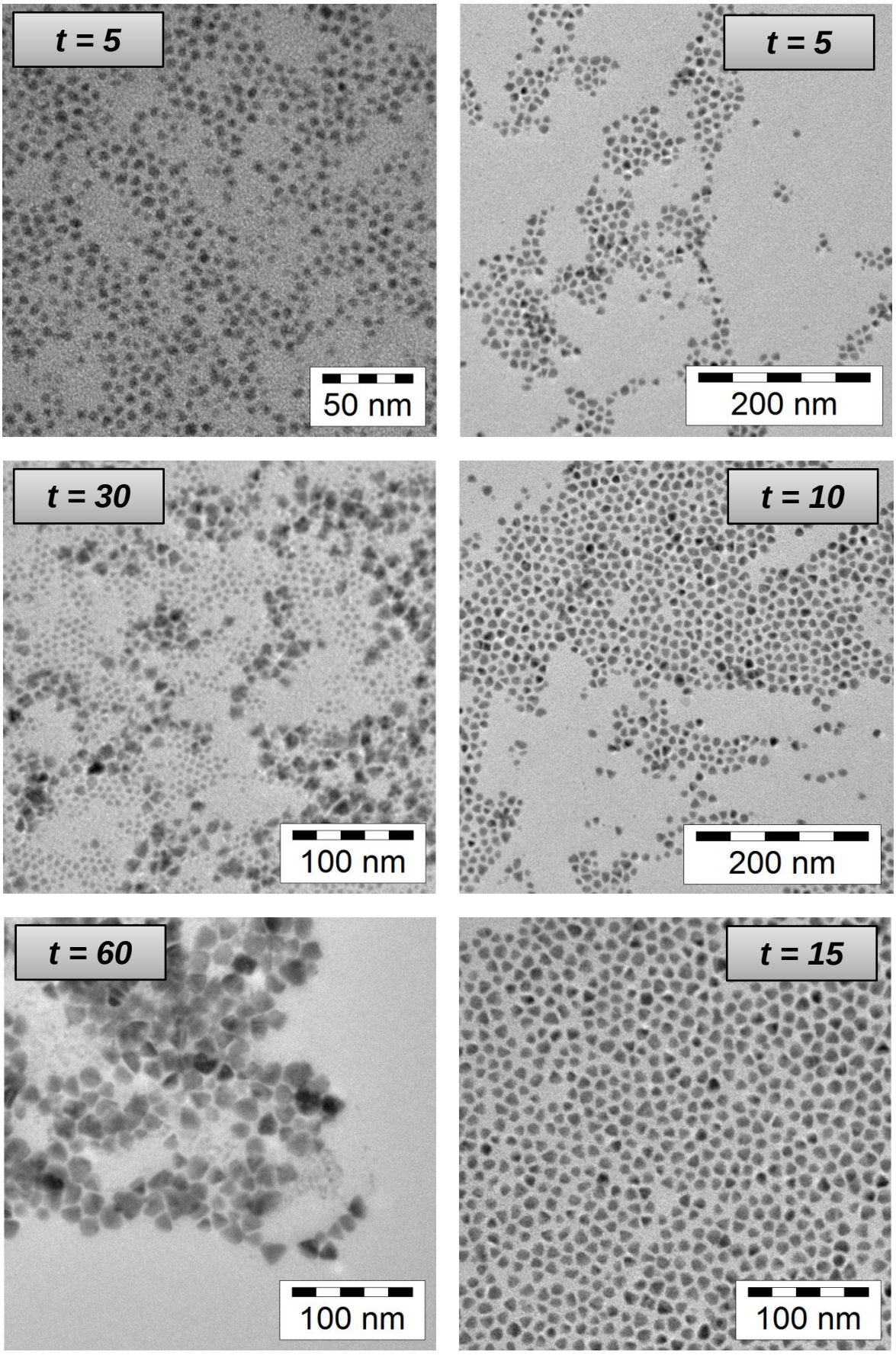

Figure 10. TEM-images of temporal evolution of [PbHg9.2]. Left column represents a 50 °C series, the right column represents 80 °C. Labels correspond to the time in minutes.

EDX-analysis was performed on [PbHg9.2_80_30], confirming that (as stated for [PbHg3_4]) the observed particles are indeed HgSe NCs (supplementary figure S27). The synthesis of HgSe NCs with defined shape is a remarkable achievement and could pave the way to the study of their optical properties as well as their assembly into a 2-dimensional superstructure.

The effect of the (Hg:Pb) ratio was investigated ([PbHg9.3B, C]). Surprisingly, increasing the ratio did not result in the formation of isotropic (triangular) particles. Results are given in table 10 and figure 11.

Table 10. Results and conditions of [PbHg9.3]

Name	T (°C)	(Pb:Hg)	Size (nm)	Shape
PbHg9.3A	RT -> 80	(1:1)	7.9 +/- 1.3	Anisotropic and Triangular
PbHg9.3B	80	(1:2)	5.6 +/- 1.0	Anisotropic
PbHg9.3C	80	(1:5)	5.3 +/- 0.9	Anisotropic
PbHg9.3D	RT	(1:1)	5.3 +/- 0.7	Spherical

[PbHg9.3D] (figure 9 D) is a control experiment to determine the effect of heating after LE and shows the expected Ostwald ripening. Figure 9A shows a TEM-image of [PbHg9.3A], clearly being more polydisperse than the sample obtained from [PbHg9.2_80] (figure 10, right column).

Comparing the different temperature profiles of [PbHg9.3A] (RT-> 80 °C), [PbHg9.2_80] (80 °C) and [PbHg9.2_50] (50 °C), it appears that a lower pre-cursor injection temperature results in higher polydispersity in the final product.

Remarkably, the TEM-images of [PbHg9.3B, C] in figure 11B,C show no formation of (2-D) triangular crystals. Thus the HgSe prisms are only observed when the (Hg:Pb) ratio is 1. This indicates there is a delicate balance between the compounds in solution; $[Se^{2-}]$:$[Pb^{2+}]$:$[Hg^{2+}]$:[OLAC]:[ODT]. Thus, the formation of (2-D) triangular HgSe would correspond to a local thermodynamic minimum. This view will be elaborated upon in section 4.3..

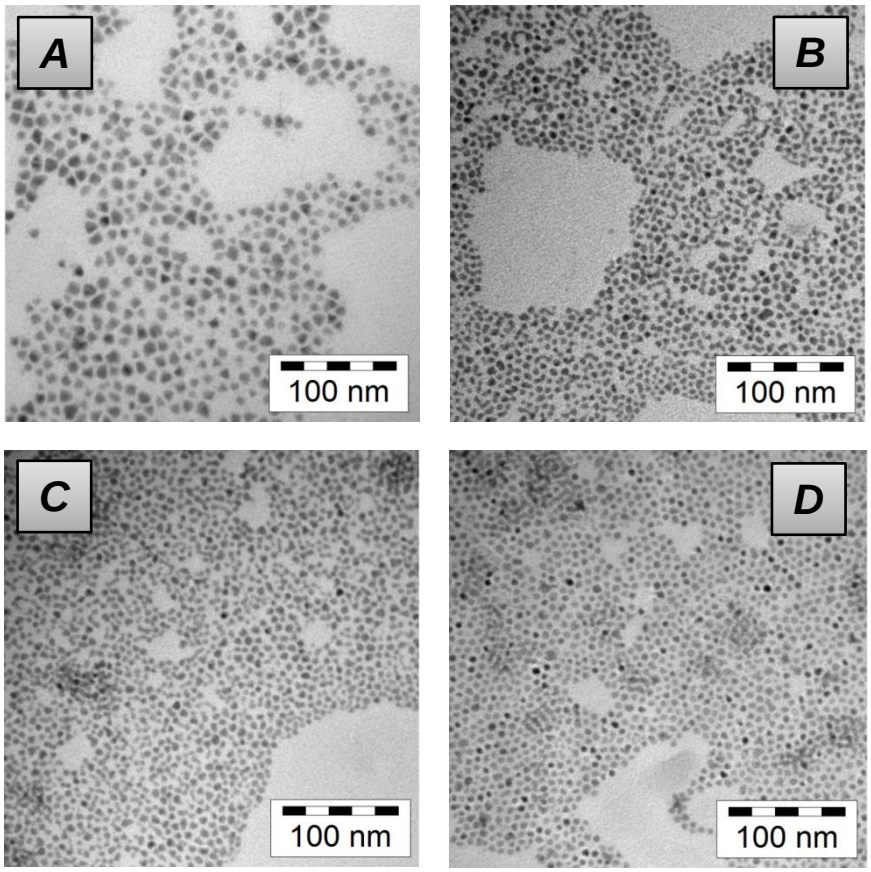

Figure 11. TEM-images of [PbHg9.3], the image labels correspond to X = A,B,C,D respectively

3.3.2. Reproducibility: [PbSe 5 nm #2,3](ODT) with [PbHg2.2]

[PbHg10, 12, 12.2, 12.3] ([PbSe 5 nm #3](ODT))

To determine the reproducibility of the results found so far, new experimental series were attempted on ODT-ligand exchanged [PbSe 5 nm #3]; [PbSe 5 nm #3](ODT). Different temperatures and amounts of ODT were tested. However, when Hg-precursor was added after the ligand exchange (and washing steps) the (2-D) triangular HgSe NCs were not formed.

[PbHg13L] ([PbSe 5 nm #2](ODT))

EDX-measurements performed on [PbSe 5 nm #1] (section 3.1.2) indicated that the PbSe NCs are surrounded by a layer of $Pb(OLAC)^+$, as reported similarly in literature[65]. For alcohols it is known that the presence of a base can induce an enormously increased ability for the $Pb(OLAC)^+$ layer to be stripped[66]. As such, considering the possibility of an impurity affecting the experimental outcome, different ligand mixtures were added to [PbSe 5 nm #2]. An overview is given in table 11. Note that batch [PbSe 5 nm #3] had been depleted and [PbSe 5 nm #2] was used.

Table 11. Ligand exchange conditions for [PbHg13L]. All quantities are in mL.

Name	PbSe 5 nm #3	Tol	ODT	Pyr	ODE	TOP	TOPO
PbHg13L_TOP	0.5	0.5	1	0.050	-	0.0100	-
PbHg13L_Pyr	0.5	0.5	1	0.050	-	-	-
PbHg13L_ODE	0.25	0.25	0.5	0.025	1	-	-
PbHg13L_TOPO	0.5	0.5	-	-	-	-	1
PbHg13L_O/T	0.25	0.25	-	-	1	-	0.5

After LE, a new experimental series, [PbHg13], was performed. Results and conditions are given in figure 12 and table 12. Note that no control experiment was performed in which only ODT was used.

Table 12. Results and conditions of [PbHg13].

Name	T (°C)	(Hg:Pb)	Size (nm)	Shape
PbHg13_TOP	80	1	8.04 +/- 1.20	Polydisperse, anisotropic, particles fused together
PbHg13_TOP2	120	1	10.74 +/- 4.95	Polydisperse, anisotropoic, particles fused together
PbHg13_Pyr	80	1	9.39 +/- 1.74	Semi-spherical with sharp interfaces, smaller material present
PbHg13_Pyr2	120	1	9.33 +/- 1.47	Semi-spherical with sharp interfaces, smaller material present
PbHg13_ODE	80	1	8.29 +/- 1.33 4.93 +/- 0.99	Large & small species of particles, both roughly spherical
PbHg13_ODE2	120	1	8.49 +/- 1.75**	NCs predominantly large spherical, few small spheres
PbHg13_TOPO	80	1	5.14 +/- 1.21	Anisotropic, aggregates present
PbHg13_TOPO2	120	1	7.53 +/- 1.30	Anisotropic, aggregates present
PbHg13_O/T	80	1	-	Aggregation (bulk?)
PbHg13_O/T2	120	1	-	Aggregation (bulk?)

**** All sizes measured as one.**

[65] Moreels et al., JACS 2008, 130, 15081
[66] Law et al., JACS 2008, 130, 5979

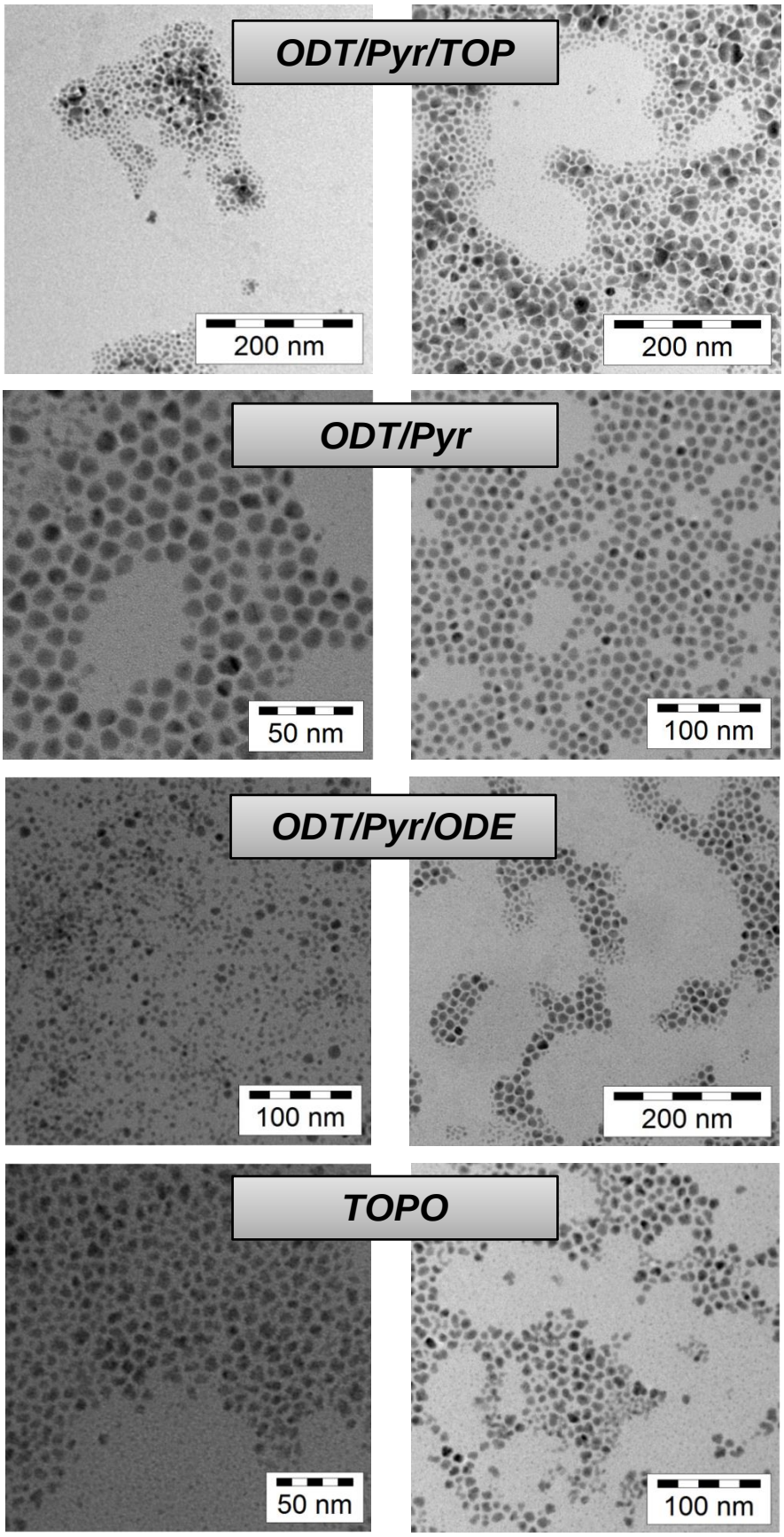

Figure 12. TEM images of [PbHg13]. The left collumn shows results of experiments performed at 80 C, the right represents experiments performed at 120 °C. The label corresponds to the ligand mixture used in the ligand exchange step.

The least polydisperse samples were analyzed with TEM-EDX, confirming the presence of HgSe (see figures 13, 14, 15).

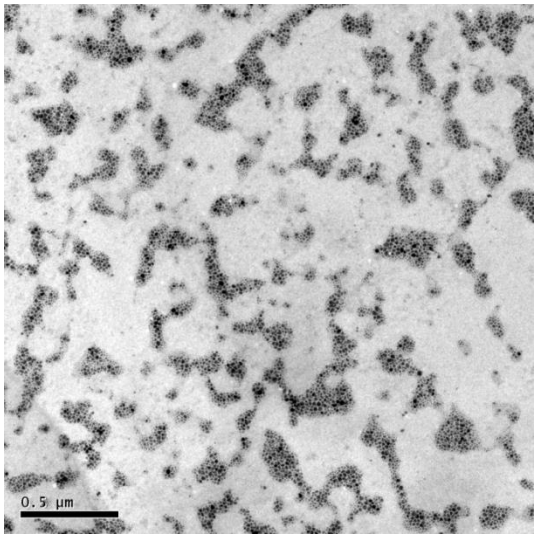

[PbHg13_TOP2]

Element	Atomic (%)	Uncertainty (%)
Se (K)	39.790	0.797
Hg (L)	46.656	1.613
Pb (L)	13.552	1.008

Figure 13. EDX-analysis of [PbHg13_TOP2]

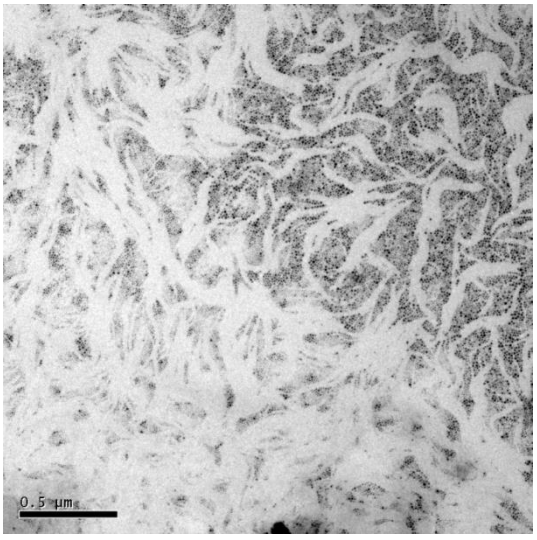

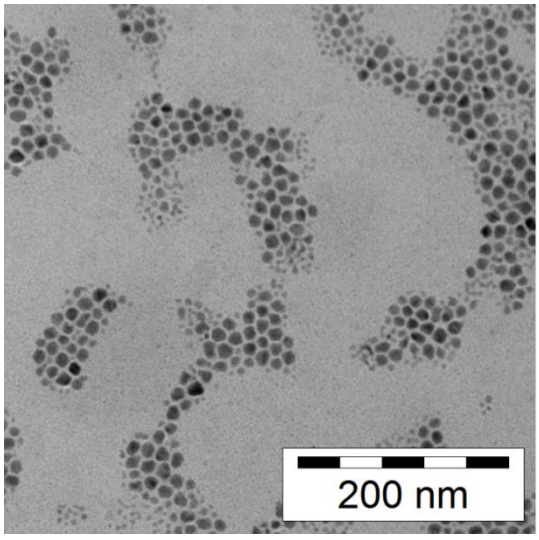

[PbHg13_ODE]

Element	Atomic (%)	Uncertainty (%)
Se (K)	38.804	0.858
Hg (L)	28.408	1.656
Pb (L)	32.786	1.634

[PbHg13_ODE2]

Element	Atomic (%)	Uncertainty (%)
Se (K)	50.760	0.985
Hg (L)	39.929	2.068
Pb (L)	9.310	1.091

Figure 14. EDX analysis of [PbHg13_ODE, ODE2]

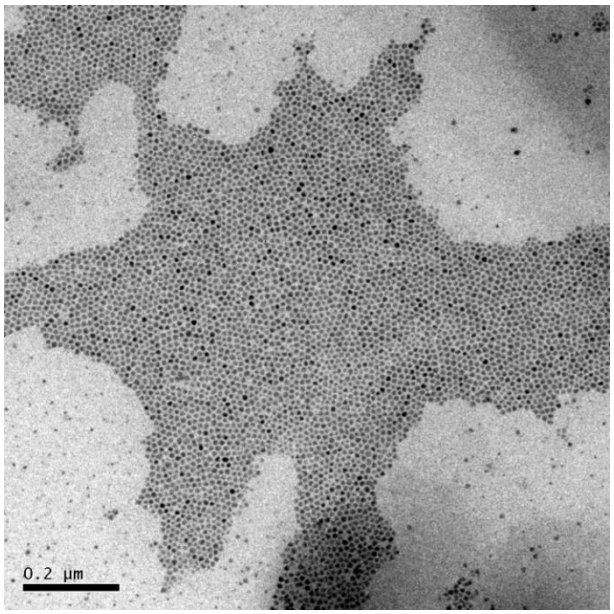

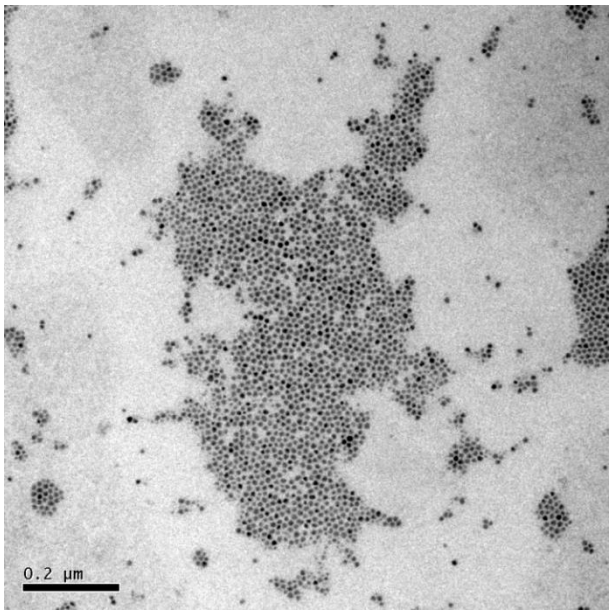

[PbHg13_Pyr] EDX1			[PbHg13_Pyr] EDX2		
Element	Atomic (%)	Uncertainty (%)	Element	Atomic (%)	Uncertainty (%)
Se (K)	46.991	0.750	Se (K)	54.957	0.956
Hg (L)	50.142	1.525	Hg (L)	38.957	1.935
Pb (L)	2.865	0.592	Pb (L)	6.085	0.843

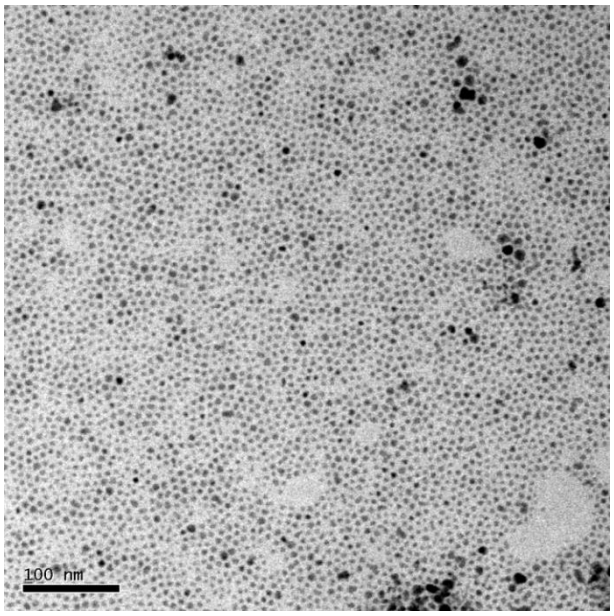

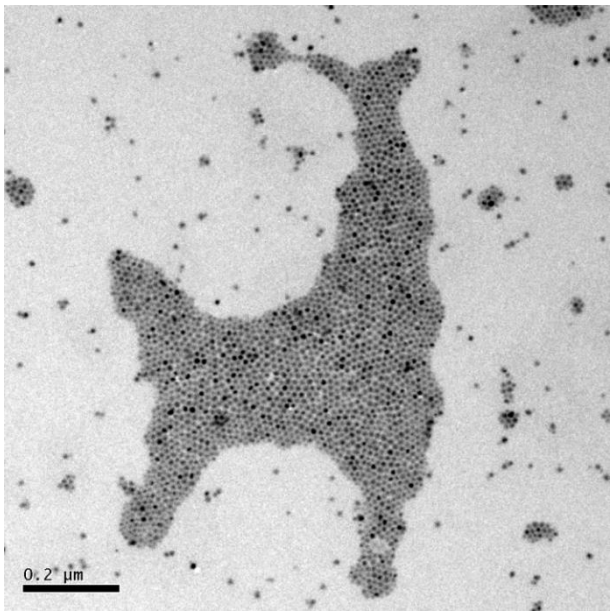

[PbHg13_Pyr2] EDX1			[PbHg13_Pyr2] EDX2		
Element	Atomic (%)	Uncertainty (%)	Element	Atomic (%)	Uncertainty (%)
Se (K)	50.438	1.233	Se (K)	49.105	0.764
Hg (L)	38.762	2.174	Hg (L)	50.894	1.600
Pb (L)	10.798	1.466	Pb (L)	~ 1	

Figure 15. EDX analysis of [PbHg13_Pyr, Pyr2]

The presented data provides a strong indication that HgSe NCs were formed. Finally the optical properties of [PbHg13_Pyr2] were shortly investigated through absorption measurements. Figure 16 shows the absorption spectrum. There is a hint of an excitonic transition at the onset of absorption around 1750 nm, but it is not clearly resolved and could be due to an underlying solvent absorption peak. The peaks above 2200 nm are solvent/ligand absorption peaks. No emission was observed.

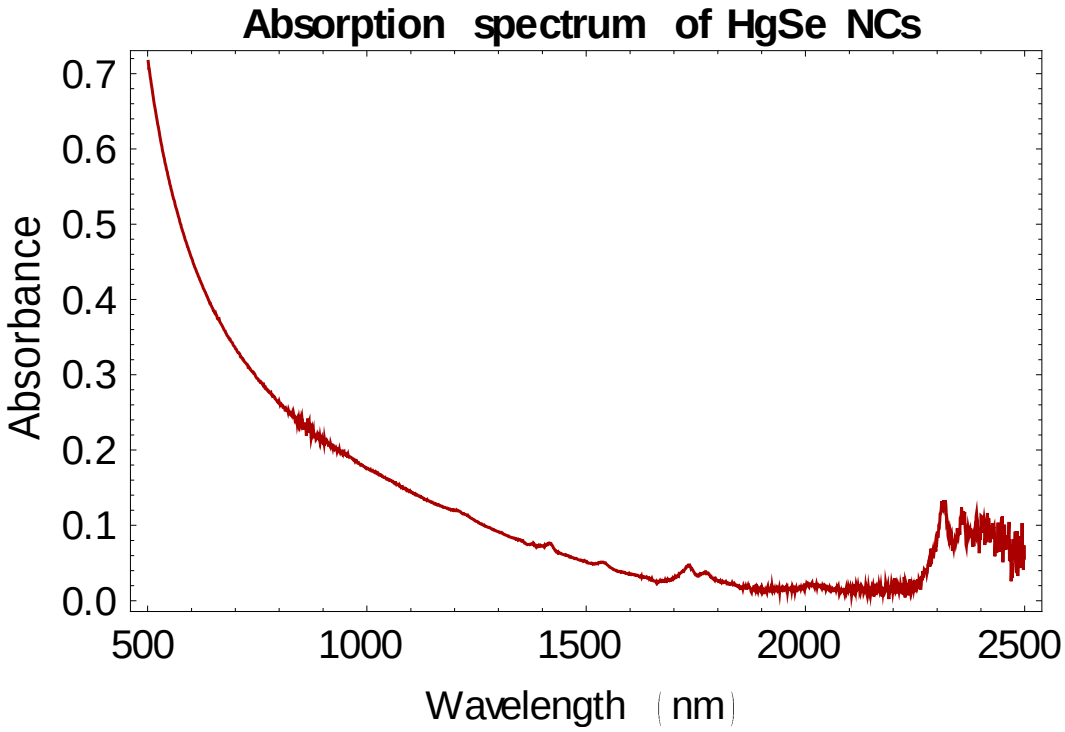

Figure 16. Absorption spectrum of [PbHg13_Pyr2].

4. Discussion

4.1. The choice of Hg-precursor and its influence on ion diffusion

As mentioned in section 1.5, the choice of ligands present in solution can strongly influence the outcome of cation exchange. In this work, different Hg-precursors have been tested. Both amines and thiols were tested in [PbHg2S, 3S], [PbHg6, 6.2], [PbHg8, 8.2], but their use did not result in the synthesis of monodisperse NCs.

When $Hg(OLAC)_2$, a carboxylic acid, was used, different amounts of both Hg and Pb were observed in the crystal phase of the final product. For example, EDX analysis of [PbHg5_EH], using the $Hg(OLAC)_2$ precursor [PreHg2.2] at a (Hg:Pb) ratio of 13.2, showed that the final product consists of ~ 15% Hg and 35% Pb (supplementary figure S19). Finding a mixed (crystal-) phase indicates that the difference in binding energy between Pb^{2+} and Hg^{2+} to oleic acid is relatively small. This is supported by the observation that the structural integrity of the original crystals is not maintained: the cations are both stable in the solution- and in the crystal phase.

Considering the relative affinities found, it is likely that, to accomplish a cation exchange of Hg^{2+}-to-Pb^{2+} with retention of the anion sublattice, a different Hg-precursor must be considered.

4.2. Ligand exchange

When a ligand exchange type reaction is performed on the PbSe NCs, one changes the surface ligand composition from PbSe(PbOLAC) to PbSe(L), where L is the ligand of choice. According to literature, when treated with different amines, surface $PbOLAC^-$ ligands can be partially removed, but are not replaced[67]. Alcohols seem to partially remove and replace the ligands[68] and using 1,2-ethanedithol (EDT), the $PbOLAC^-$ ligands can be removed and replaced (almost) completely[69].

It is likely that ODT is similarly able to remove and replace $PbOLAC^-$ from the surface. However the discrepancy between and difficulties in reproducing earlier results from [PbHg9] to [PbHg13], suggest that a LE-type reaction does not always result in the same composition of surface ligands – even when an excess of to-be-exchanged-ligand is present. As one batch of ODT was finished and replaced by a new one, a possible explanation can be the presence of an impurity or contamination in the ODT.

Assuming there is a driving force resulting from the equilibrium between ligands on the surface of the NCs and in solution, the success of pyridine addition points to its role as co-ligand. This role as catalyst in ligand exchange and / or $PbOLAC^-$ stripping can be attributed to either or both of the following mechanisms:

a. Facilitating the de-coordination of ligands at the NC-surface.
b. Playing a role as chemical activator through the (de-)protonation of ligands in solution. (Note that this de-protonation generated nucleophiles *in situ*. However, it is unlikely that ODT^- will perform a nucleophilic attack on the δ^+-carbon of the oleic acid carboxylate moiety.)

[67] Law et al., JACS 2008, 130, 5979
[68] Hassinen et al., JACS 2012, 134, 20705
[69] Luther et al., ACS Nano 2008, 2, 271

The role of pyridine in the case of [PbHg13] as chemical activator would be through its basic nature; it deprotonates the ODT in solution, thereby shifting the equilibrium towards the exchange of $PbOLAC^-$ for ODT^-. Furthermore the small size of the pyridine molecule could enable it to more effectively pass the steric barrier formed by the OLAC-alkyl-chains, thereby lowering the kinetic barrier for $PbOLAC^-$ dissociation. This shows how PbSe NCs deviate in behavior from for example CdTe[70] or CdSe[71] where the kinetic barrier for LE is lower due to the absence of a Pb-adatom layer. In this view a contamination would be present during the ligand exchange performed prior to [PbHg9].

** It has to be mentioned that while addition of "pure" ODT worked on [PbSe 5 nm #1] (with respect to HgSe formation), it did not work on [PbSe 5 nm #3] with a new batch of ODT. However, while using that same new batch of ODT worked on [PbSe 5 nm #2] in the presence of pyridine, no control experiment using only ODT was performed.

4.3. Oleic acid as solvation framework for solution-to-crystal phase transitions

Experiments [PbHg2,3,4,5,7] and [PbHgSheet] provide a strong indication that the addition of $Hg(OLAC)_2$ causes removal of both Pb^{2+} and Se^{2-} from the surface of the PbSe NCs after which it can form HgSe or PbSe/HgSe NCs. It is unclear how this process proceeds. Possibly, Hg^{2+}-cations are initially exchanged for Pb^{2+} through a vacancy at the surface, but return to solution as [Hg-Se]-monomers stabilized by ligands. This cation-exchange-facilitated etching continues until the NCs have reached a critical size (~3.8 nm) and a steady state equilibrium is established. Another option mentioned by Wark et al. is that fragmentation occurs due to build-up of strain at the hetero-interface[72]. However, due to the similar lattice constants of HgSe and PbSe (0.608 [73] and 0.6126 [74] nm in the bulk respectively), this is deemed unlikely.

Re-nucleation can occur in solution, but it is improbable that the system will become supersaturated with respect to the presence of both Pb or Hg and Se in solution. Most probably [HgSe]-monomers can re-nucleate on the etched particles and thus proceed to form HgSe NCs in a process where the original PbSe NCs are consumed. A full conversion to HgSe is observed at high cation ratio (40) for [PbHg1] and a material of mixed composition was obtained for [PbHg5_EH] (ratio = 13.2). How can the formation of HgSe NCs in post-LE-reactions then be explained?

A straightforward explanation is to consider the ratio of $[Pb^{2+}]$: $[Se^{2-}]$: $[Hg^{2+}]$. If the EDX-measurements performed on [PbSe 5 nm #1] are taken to be correct and if it is assumed that after ligand exchange the ratio of (Pb:Se) is close to 1, the experimental results can be summarized as:

Table 13. Relative crystal component ratio's

Before ligand exchange	$[Pb^{2+}]$	$[Se^{2-}]$	$[Hg^{2+}]$	Monodisperse HgSe NCs?
(Hg:Pb) = 1	3	2	2	No
(Hg:Pb) = 5	3	2	5	No
(Hg:Pb) = 40	3	2	40	No
After ligand exchange				
(Hg:Pb) = 1	1	1	1	Yes
(Hg:Pb) = 5	1	1	5	No

[70] Wuister et al., Nano Lett. 2003, 3, 503
[71] Koole et al., ACS Nano 2008, 2, 1703
[72] Wark et al., JACS 2008, 130, 9550
[73] Jayaraman et al., Phys. Rev. 1963, 130, 2277
[74] Wolfe, "Physical Properties of Semiconductors", Prentence Hall ,New York, 1989

Here the concentration of oleic acid has not been taken into account since it is added in large excess (see table 3, section 3.1.4.). This indicates that there is a delicate balance for HgSe formation corresponding to a local thermodynamic equilibrium. Herein OLAC functions as both capping agent and solution ligand, effectively forming the solvation framework through which phase transitions from solvent to crystal and back can occur (see figure 17). This view is corroborated by the observation that the difference between the relative binding strengths of both Hg^{2+} and Pb^{2+} to oleic acid appears to be small (section 4.1.).

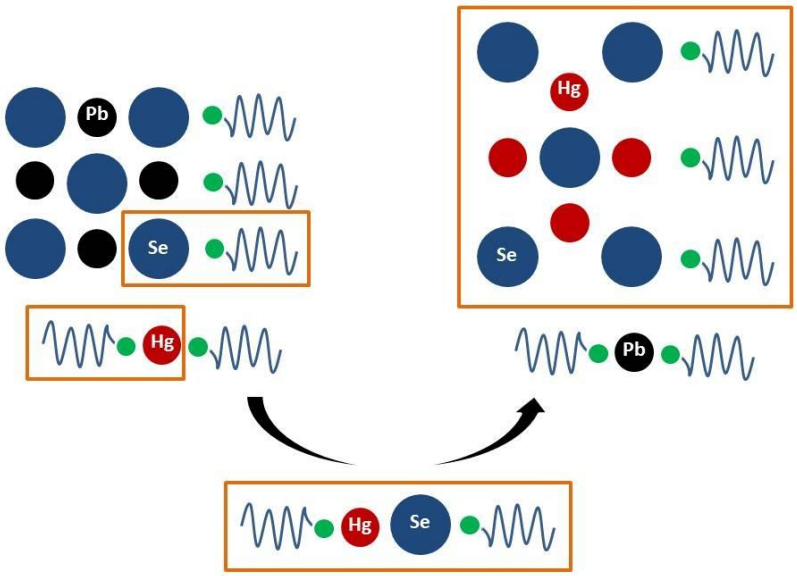

Figure 17. Schematic representation of HgSe formation

In literature this mechanism is referred to as "digestive ripening"[75]. The system is ideally suited for HgSe formation if the ratio of (Hg:Pb:Se) = 1. Upon Hg-precursor addition a very fast temperature dependent stripping and nucleation event is triggered eventually resulting in the formation of HgSe NCs. This temperature dependence is evident from the differences in sample polydispersity (section 3.3.1.) and points to a kinetic barrier towards HgSe formation.

What is still unclear is the role of ODT, which should have a higher affinity to Hg^{2+} than OLAC, at least compared to Pb^{2+}. Furthermore it has to be noted that no control experiment has been performed to confirm the importance of the Pb:(Hg:Se) ratio or the Se:(Hg:Pb) ratio (in which $Pb(OLAC)_2$ or Se would have to be added).

Now a possible explanation for the formation of the (2D-)triangular shaped NCs in [PbHg3_4] can be given. In this experiment no ligand exchange was performed prior to $Hg(OLAC)_2$ addition. However, due to problems during the purifications, the sample was heated *after* alcohols had already been added as anti-solvent. Thus, the thermodynamic equilibrium of the system has already been shifted due to the presence of alcohols. But this cannot be the only factor since many attempts have been made to reproduce the experimental conditions ([PbHg3.3, 7, 7.2]). A possible explanation can be found considering a contamination such as the presence of a base, which can catalyze nucleophilic attack of alcohols to carboxylic acids[76]. This could shift the equilibrium towards preferential solvation of Pb^{2+}. However, it has to be mentioned that no hard proof exists and again control experiments where the composition of the solution is determined (through NMR, MS etc.) would have to be performed.

[75] Samia et al., JACS 2005, 127, 4126
[76] Warren, Clayden & Greeves, "Organic Chemistry" 2nd ed., Oxford University Press, 2012

4.4. Ligand exchange using mixed ligands

Ligand exchange in the presence of selenium-binding co-ligands was attempted in order to impair control over dissolution and re-nucleation of species in solution. Their choice was based on reported affinity to selenium[77]. Crystals obtained after Hg-precursor addition resulted in NCs which differ, mainly in terms of the size dispersion of HgSe NCs and the amount of PbSe NCs present. Analysis of TEM-images presented in figure 12 provides an intuitive insight in the underlying mechanisms.

ODE (PbHg13_ODE, ODE2)
ODE was used as co-ligand for Se, having in mind its ability to solubilize Se would provide an additional driving force for the dissociation of $PbOLAC^-$ from the PbSe surface. However, due its weak coordinating nature (heating for 2 hours at 200 °C required for dissolution compared to 10 minutes at 80 °C for TOP=Se) it is possible that ODE had no role as (Se) coordinating ligand in the presence of both ODT, (OLAC) and pyridine, only serving as dilutant. The difference to [PbHg13_Pyr, Pyr2] is then simply the efficiency with which the $PbOLAC^-$ was removed.

TOP (PbHg13_TOP, TOP2)
TOP was used with a similar goal in mind, although the obtained results are mechanistically far more interesting: the obtained crystals are very polydisperse. Considering the effective binding of TOP to Selenium it is very clear that this binding changes the reaction outcome for the formation of HgSe NCs. Most likely the supply of Se-monomers for HgSe NCs formation is (either much faster, or) much slower than the availability of Hg^{2+}. In this case, all "free" Se-monomers are immediately consumed (kinetic effect). Furthermore, the association of TOP with Selenium on the surface of HgSe prevents digestive ripening to an equilibrium shape. To obtain a less polydisperse sample and to verify this hypothesis (at least concerning TOP), the synthesis should be carried out at higher temperature.

TOPO
The results obtained using TOPO are inconclusive. At 80 °C the experimental results resemble those of particles obtain in a non-ligand exchanged reaction in shape, although the particles are bigger on average. At higher temperatures, the particles grow even further in size, but are very anisotropic. As no EDX-measurements were performed on this sample, no clear conclusions can be drawn.

4.5. Comparison to earlier work on HgSe

As mentioned in section 1.5, earlier work has been performed on the synthesis of HgSe NCs. After the initial work in the group of Weller and reports on HgSe clusters by Kuno et al. the work was renewed in 2008 by Howes and coworkers. They synthesized both spherical and triangular HgSe NCs and reported on digestive ripening inducing a reduction in average size from 4.9 nm to 3.8 nm. However, the material was optically inactive, showing no emission and lacking any characteristic excitonic features in the absorption spectrum[78]. Despite the similarities between their results and the results obtained in this research, it is clear from the TEM-images that the NCs obtained during this work are less polydisperse and more efficiently capped with ligands (i.e. the NCs are lie separated on the carbon substrate of the TEM-grid) (figure 18). In fact, they show closer resemblance to the HgSe NCs synthesized by Keuleyan et al. that showed efficient narrow emission (figure 19) [79].

[77] Jasieniak et al., J. Phys. Chem. B. 2005, 109, 20665
[78] Howes et al., J. Mater. Chem. 2008, 18, 3474
[79] Keuleyan et al., JACS 2011, 133, 16422

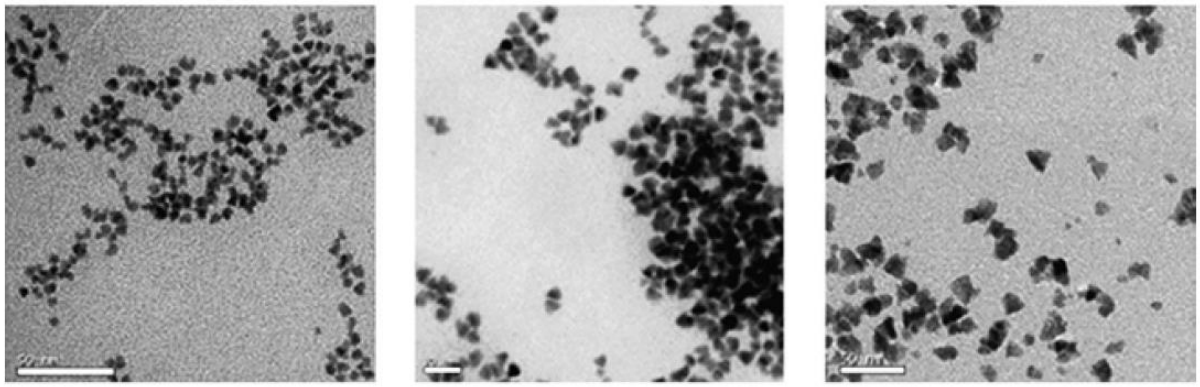

Figure 18. TEM-images of HgSe NCs prepared by Howes et al. through different synthesis methods. Scale bars represent 50 nm.

Considering the current state of the research, the HgSe NCs synthesized compare well to larger crystals synthesized by others. Future research will have to show whether we will be able to study and, more importantly, utilize these (large)(monodisperse) HgSe QDs in their promising applications.

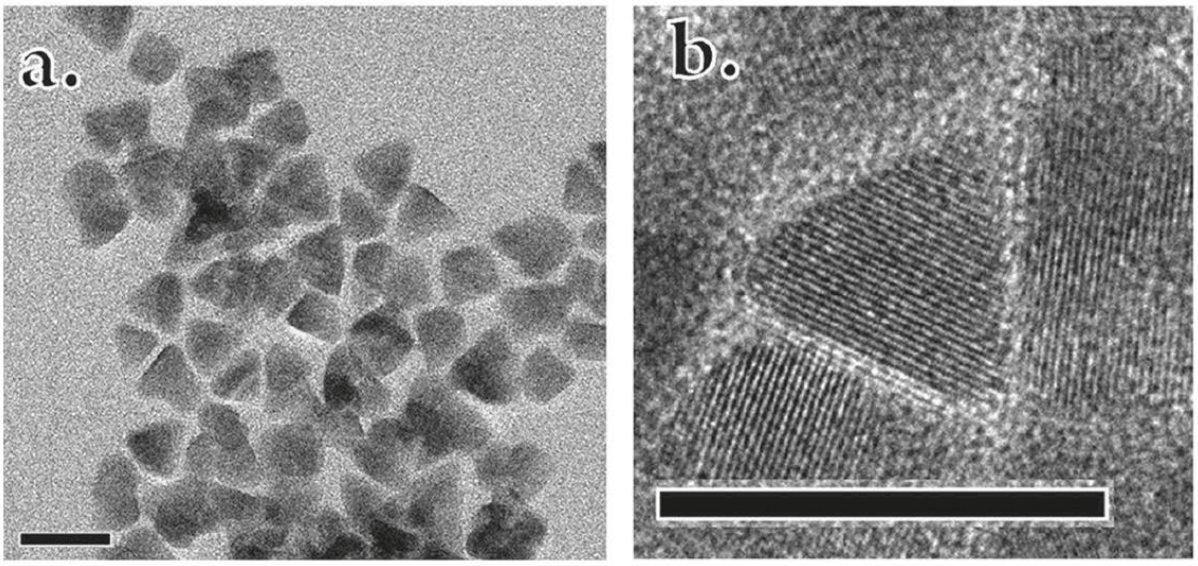

Figure 19. a) TEM-image of HgTe NCs obtained by Keuleyan et al.;
b) HR-TEM images of the same crystals.

5. Conclusions

The single cation exchange reaction of Pb-to-Hg on PbSe NCs has been investigated over a range of temperatures, reaction times, cation ratio's and precursor compositions (oleic acid, ethylene glycol, amines, thiols and their mixtures). The conversion of PbSe to HgSe with conservation of shape and size was not observed. However, the transformation of PbSe NCs into HgSe NCs has been found to occur through a process of digestive ripening.

The formation of 4 nm HgSe NCs occurs at high Hg-to-Pb ratio. Under specific conditions, prism-shaped HgSe NCs of 9 nm with small size dispersion were formed. The replacement of Pb-oleate surface ligands by ligand exchange using octadecanethiol and pyridine prior to Hg-precursor injection was found to be an important step for the synthesis of these prism-shaped NCs. Furthermore, the ratio of Hg-to-Pb-to-Se has to be close to 1. The role of oleic acid is that of a solvation framework for the solution-to-crystal phase transitions of PbSe and HgSe.

Many studies have focused on HgTe and its alloys. Eventhough the application of HgSe as IR-active material and as topological insulator has been theorized, the lack in synthetic knowledge has hampered the study of its potentially extraordinary electronic properties. The 9 nm prism shaped HgSe NCs surpass literature reports in terms of size and shape dispersion, paving the way for their assembly into 2-dimensional super-structures and eventual application in devices.

6. Perspectives

The current state of solvo-chemical HgSe NC synthesis leaves “plenty of room” for further investigation. As indicated throughout this work, research could advance towards one or more of the categories presented below.

6.1. Synthesis optimization

The synthesis could be further optimized in terms of:

I. Method of $PbOLAC^-$-removal prior to Hg-precursor addition. Full removal can be achieved by utilization of Meerwein’s salt[80] or multiple cycles of addition of other ligands such as alcohols and/or amines. In any case, full or partial removal of the $PbOLAC^-$ layer will provide valuable information on the ideal (Pb:Hg:Se) ratio.

II. Solvent composition during the reaction. As was observed for [PbHg3_4], triangular HgSe NCs can be formed by changing solution phase equilibrium *in situ*. From a mechanistic, digestive ripening point of view, It should be very interesting to test the effect of different solvent-solvent or ligand-solvent compositions (possibly with the eventual goal of obtaining a phase diagram which provides insight into the facile manipulation of the reaction mixture to obtain a desired crystal composition) .

III. The effect of increasing the Se:(Hg:Pb) or Pb:(Hg:Se) ratio where the (Hg:Pb) and (Hg:Se) both equal 1, for example by means of adding TOP=Se, Se dissolved in ODE or $Pb(OLAC)_2$.

6.2. Optical properties

Measuring narrow band photoluminescence is what would validate this new synthesis method. Short investigation of the optical properties revealed no clearly distinguishable excitonic features in the optical density profile and no observed emission. Therefor it is imperative to thoroughly evaluate the effect of post-synthetic treatment of the NCs. Surface traps may be present due to insufficiently passivating ligands at the NC surface. One option may be the addition of TOP and ODT as used by Keuleyan et al. in the synthesis of HgTe[81]. Alternatively, shell over-growth of the lattice matched CdSe may be attempted analogues to the approaches taken in the group of Weller[82], profiting from advances in research performed since their publication in 2000[83].

6.3. Alternative cation exchange routes

In this work different precursor chemistry (carboxylic acid, amines, thiols, alcohols) has been investiged to accomplish a ion exchange process for Pb-to-Hg exchange in PbSe NCs. Although none of the tested ligands was successful in terms of direct exchange, sequential cation exchange, using the popular Cu(I) as intermediate may be a viable alternative (see Appendix F).

[80] Rosen et al., Angew. Chem. Int. Ed. 2012, 51, 684
[81] Keuleyan et al., JACS 2011, 133, 16422
[82] Harrison et al., Pure Appl. Chem. 2000, 72, 295
[83] Lee et al., JACS 2010, 132, 9960

7. List of references according to footnotes

** Note that some references are listed more than once.

[1]. De Mello Donegá, Chem. Soc. Rev. 2011, 40, 1512
[2]. Hughes et al., ACS Nano 2012, 6, 4573
[3]. Talapin et al., Chem. Rev. 2010, 110, 389
[4]. http://www.nature.com/news/quantum-dots-go-on-display-1.12216 (visited January 29th 2013)
[5]. Roduner, Cronin, "Nanoscopic Materials: Size-Dependent Phenomena", Wiley 2006
[6]. Smith et al., Acc. Chem. Res. 2010, 43, 190
[7]. Casavola et al., Nano Lett. 2009, 9, 366
[8]. Son et al., Science 2004, 306, 1009
[9]. Stoeva et al., Langmuir 2005, 21, 10280
[10]. Schaaf et al., J. Phys. Chem. B 1999, 103, 9394
[11]. Smetana et al., J. Phys. Chem. B 2006, 110, 2155
[12]. Lin et al., J. Nanop. Res. 2002, 2, 157
[13]. Rongchao et al., JACS 2004, 126, 9900
[14]. Samia et al., JACS 2005, 127, 4126
[15]. Hines et al., Adv. Mater. 2003, 15, 1844
[16]. Jain et al., JACS 2010, 132, 9997
[17]. Miszta et al., ASC Nano 2011, 9, 7176
[18]. Kovalenko et al., Angew. Chem. Int. Ed. 2008, 47, 3029
[19]. Shriver and Atkins, "Inorganic Chemistry" 4th ed., Oxford University Press
[20]. Luther et al., JACS 2009, 131, 16851
[21]. Wark et al., JACS 2008, 130, 9950
[22]. Rivest et al., Chem. Soc. Rev. 2013, 42, 89
[23]. Li et al., Nano Lett. 2011, 11, 4964
[24]. Robinson et al., Science 2007, 317, 355
[25]. Pietryga et al., JACS 2008, 130 (14), 4879
[26]. Casavola et al., Chem. Mat. 2012, 24, 294
[27]. Murray et al., JACS 1993, 115, 8705
[28]. Wehrenberg et al., J. Phys. Chem. B 2002, 106, 10634
[29]. Rogach et al., Adv. Mater. 1999, 11, 552
[30]. Harrison et al., Pure Appl. Chem. 2000, 72, 295
[31]. Higginson et al., J. Phys. Chem. B 2002, 106, 9982
[32]. Kuno et al., J. Phys. Chem. 2003, 107, 5758
[33]. Li et al., J. Phys. & Chem. of Sol. 1999, 60, 965
[34]. Yang et al., J. Mater. Res. 2002, 17, 1147
[35]. Ding et al., Mater. Lett. 2003, 57, 4445
[36]. Kane & Moore, *Physicsworld*, February 2011, 32
[37]. Qi et al., Phys. Rev. B 2006, 74, 085308
[38]. Qi et al., Physics Today Jan. 2010, 33
[39]. Murakami et al., Phys. Rev. Lett. 2004, 93, 156804-1
[40]. He and Sun, High-k Gate Dielectrics for CMOS Technology, Wiley 2012, 1st Ed.
[41]. König et al., Science 2007, 213, 766
[42]. Hasan et al., Rev. Mod. Phys. 2010, 82, 3045
[43]. Evers et al., Nano Lett. 2012, ASAP
[44]. Lui et al., Nano lett. 2011, 11, 5349
[45]. Steckel et al., JACS 2006, 128, 13032
[46]. Evans et al., JACS 2010, 132, 10973
[47]. Moreels et al., Chem. Mater. 2007, 19, 6101
[48]. Casavola et al., Chem. Mater. 2012, 24, 294
[49]. Pietryga et al., JACS 2008, 130, 4879
[50]. Smith et al., JACS 2011, 133, 24
[51]. Keuleyan et al., JACS 2011, 133, 16422
[52]. Physical Chemistry – D.W. Ball, Thomson Learning, Brooks/Cole 2003
[53]. Smith et al., JACS 2011, 133, 24
[54]. Son et al., Science 2004, 306, 1009
[55]. Wolfe, "Physical Properties of Semiconductors", Prentence Hall ,New York, 1989

[56]. Jayaraman et al., Phys. Rev. 1963, 130, 2277
[57]. Evers et al., Nano Lett. 2012, ASAP
[58]. R.D. Shannon, Acta Cryst. 1976, A 32, 751
[59]. Wang et al., Dalton Tran. 2012, 41, 12726
[60]. Lingley et al., Nano Lett. 2011, 11, 2887
[61]. Hoffmann et al., Inorg. Chem. 2001, 40, 977
[62]. Canty et al., Inorg. Chim. Acta 1977, 24, 109
[63]. Bochmann et al., J. Chem. Soc. Dalt. Trans. 1991, 2325
[64]. Keuleyan et al., JACS 2011, 133, 16422
[65]. Moreels et al., JACS 2008, 130, 15081
[66]. Law et al., JACS 2008, 130, 5979
[67]. Law et al., JACS 2008, 130, 5979
[68]. Hassinen et al., JACS 2012, 134, 20705
[69]. Luther et al., ACS Nano 2008, 2, 271
[70]. Wuister et al., Nano Lett. 2003, 3, 503
[71]. Koole et al., ACS Nano 2008, 2, 1703
[72]. Wark et al., JACS 2008, 130, 9550
[73]. Jayaraman et al., Phys. Rev. 1963, 130, 2277
[74]. Wolfe, “Physical Properties of Semiconductors”, Prentence Hall ,New York, 1989
[75]. Samia et al., JACS 2005, 127, 4126
[76]. Warren, Clayden & Greeves, “Organic Chemistry” 2nd ed., Oxford University Press, 2012
[77]. Jasieniak et al., J. Phys. Chem. B. 2005, 109, 20665
[78]. Howes et al., J. Mater. Chem. 2008, 18, 3474
[79]. Keuleyan et al., JACS 2011, 133, 16422
[80]. Rosen et al., Angew. Chem. Int. Ed. 2012, 51, 684
[81]. Keuleyan et al., JACS 2011, 133, 16422
[82]. Harrison et al., Pure Appl. Chem. 2000, 72, 295
[83]. Lee et al., JACS 2010, 132, 9960
[84]. X-ray absorption edges: http://www.med.harvard.edu/jpnm/physics/refs/xrayemis.html
[85]. Li et al., Nano lett. 2011, 11, 4964
[86]. Mohamed et al., J. Phys. Chem. B 2005, 109, 10533-10537
[87]. Rivest et al., Chem. Soc. Rev. 2013, 42, 89

Appendix A: Supplementary Figures

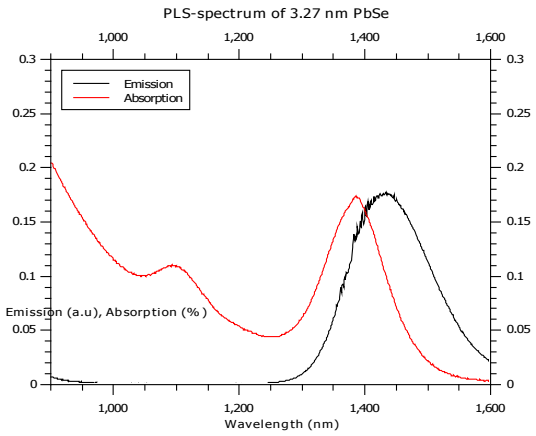

Figure S- 1. Optical measurements of [PbSe 3.3 nm]

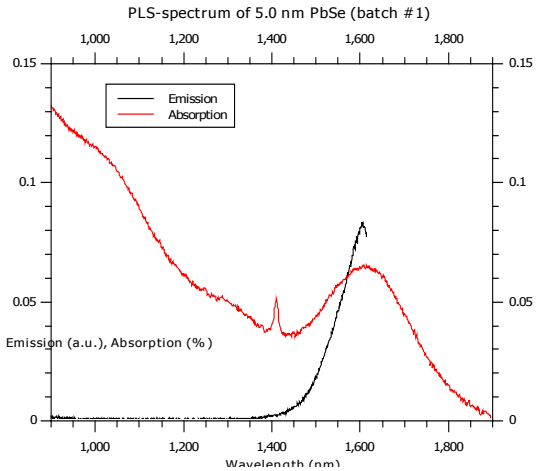

Figure S- 2. Optical measurements of [PbSe 5 nm #1]

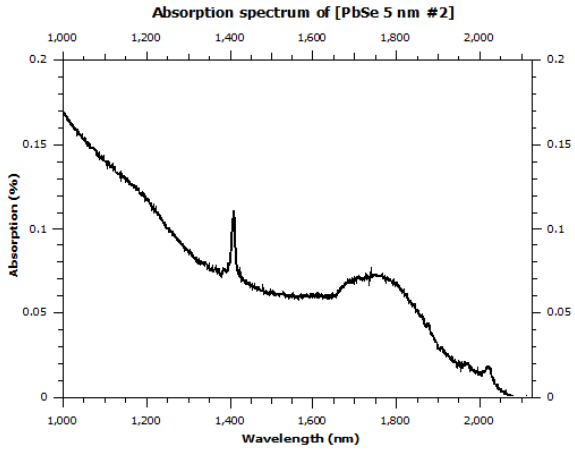

Figure S- 3. Absorption spectrum of [PbSe 5 nm #2]

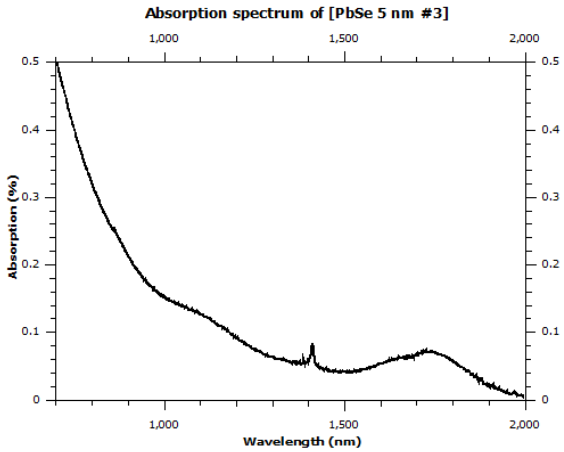

Figure S- 4. Absorption spectrum of [PbSe 5 nm #3]

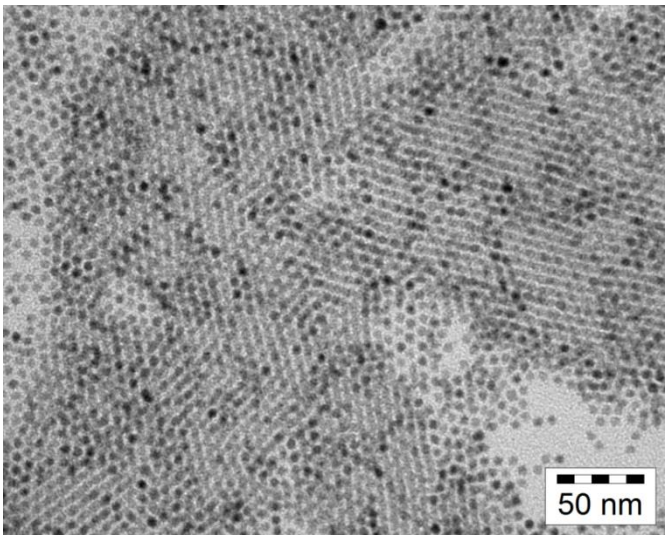

Element	Atomic (%)	Uncertainty (%)
Se (K)	41.630	0.484
Pb (L)	58.369	1.216

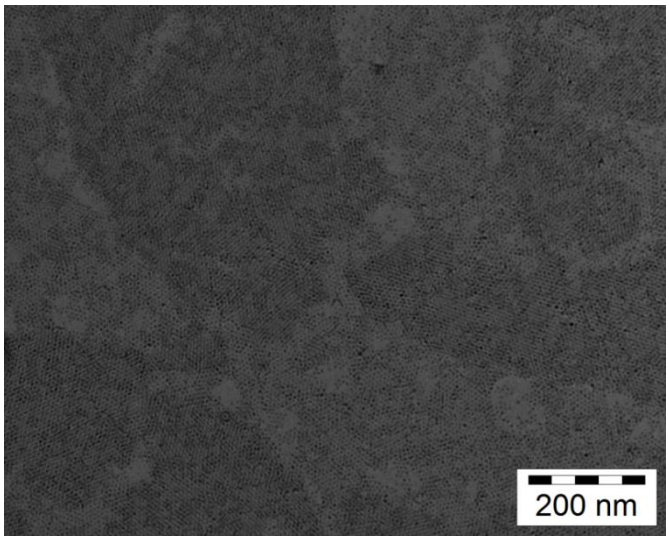

Element	Atomic (%)	Uncertainty (%)
Se (K)	37.412	0.515
Pb (L)	62.587	1.317

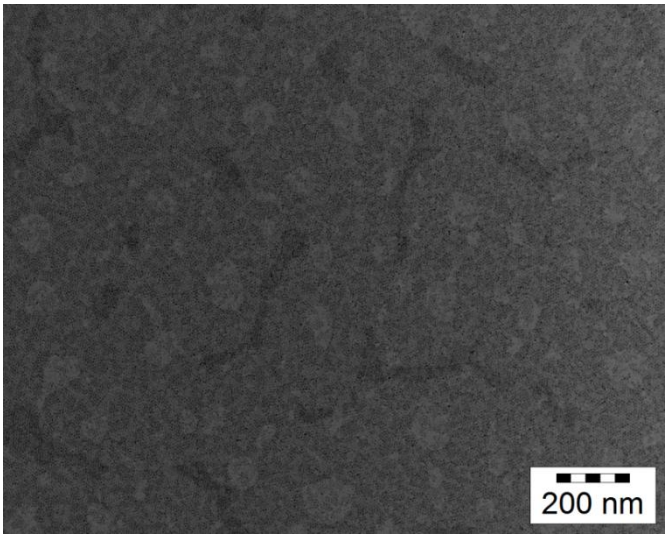

Element	Atomic (%)	Uncertainty (%)
Se (K)	39.114	0.578
Pb (L)	60.885	1.549

Figure S- 5. EDX-analysis of [PbSe 5 nm #1]

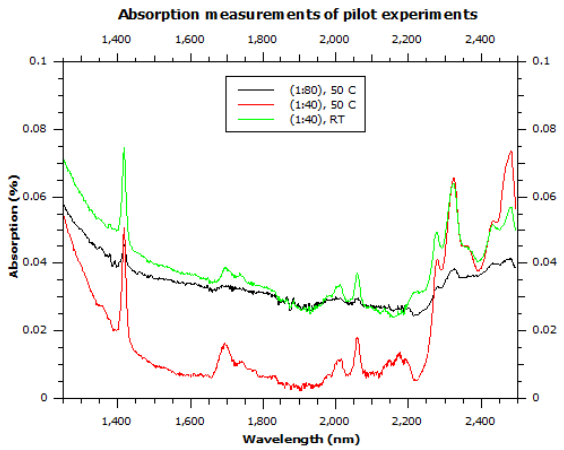

Figure S- 6. Absorption spectra of pilot experiments

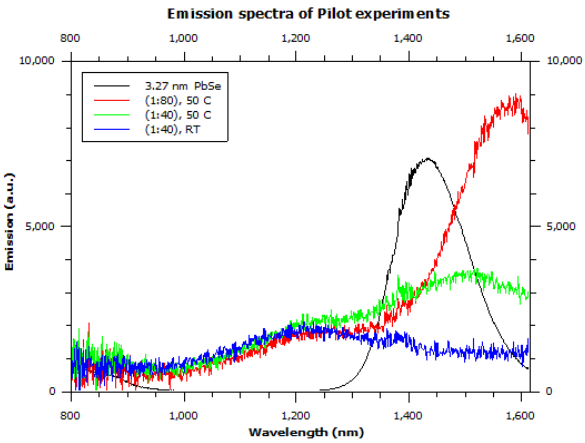

Figure S- 7. Emssion spectra of pilot experiments

* It is hard to relate the spectra in figure S6 and S7 to any expected optical behavior of the HgSe NCs.
  - The absorption measurements are dominated by solvent peaks.
  - The emission spectra have very low signal. Further, although the first peak at 1200 nm may be related to QD-emission it is very poorly resolved. The peak coming up at ~ 1500 nm cannot be assigned due to its absence in the first sample (which also showed a color change at the initial injection).

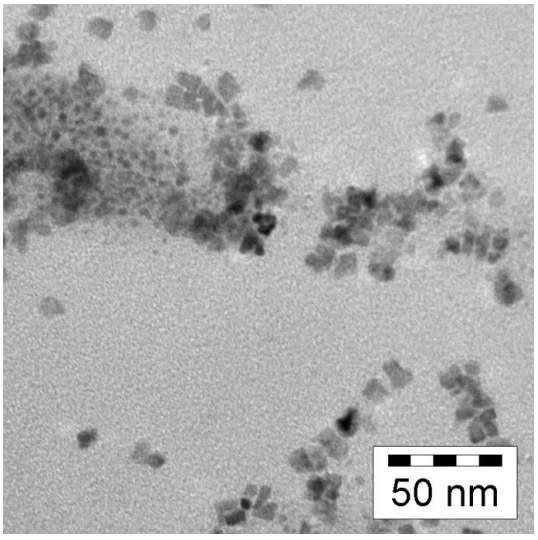

Figure S- 8. TEM-image of [PbHg2_-10]

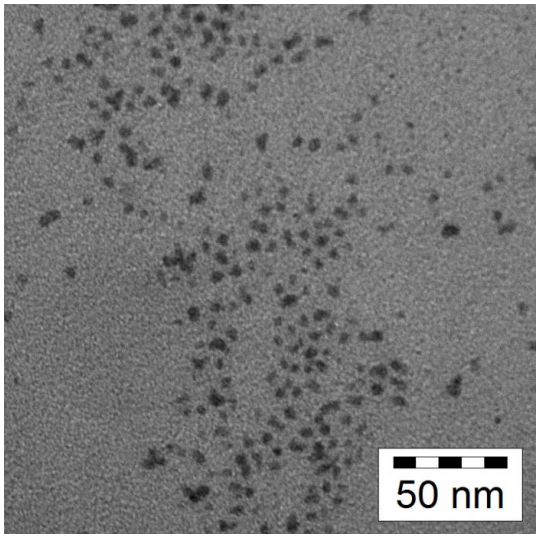

Figure S- 9. TEM-image of [PbHg2_RT]

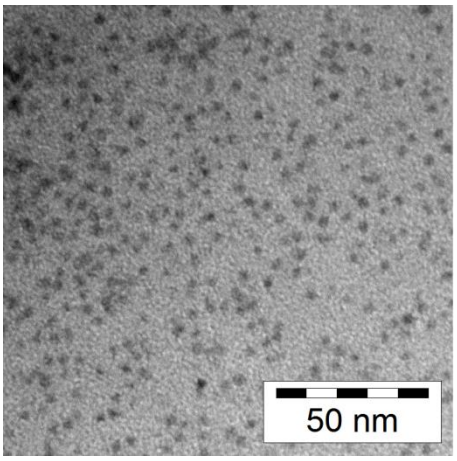

Figure S- 10. TEM image of [PbHg2S_4]

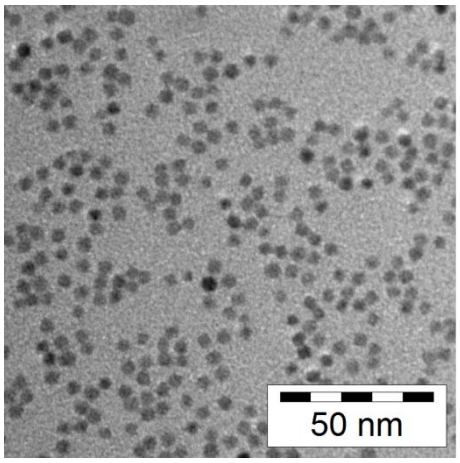

Figure S- 11. TEM image of PbHg3S_1

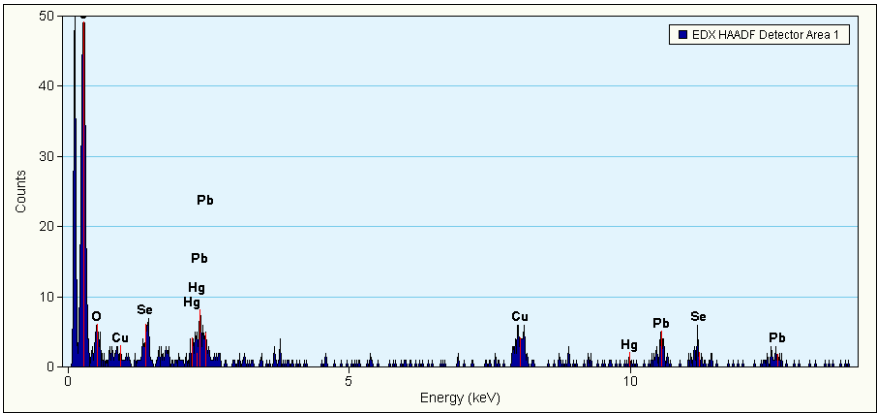

Figure S- 12. TEM-EDX spectrum (1) of PbHg3S_1

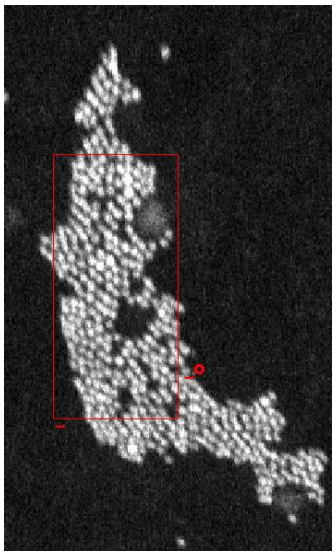

Figure S- 13. HAADF image corresponding to TEM-EDX(1) of PbHg3S_1

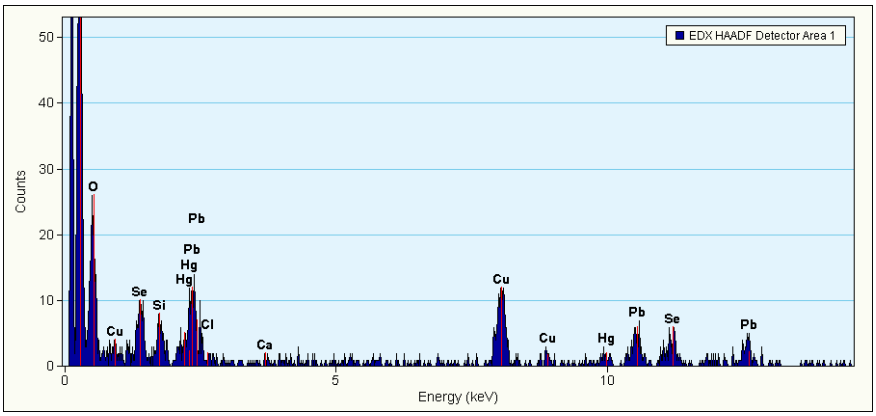

Figure S- 14. TEM-EDX spectrum (2) of PbHg3S_1

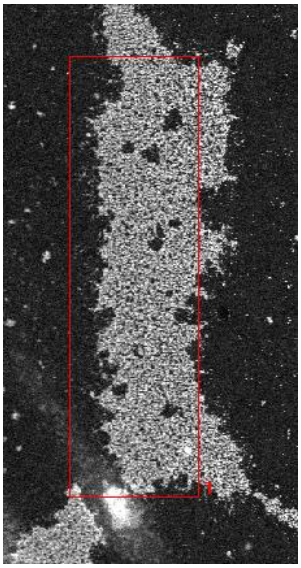

Figure S- 15. HAADF image corresponding to TEM-EDX(2) of PbHgS3_1

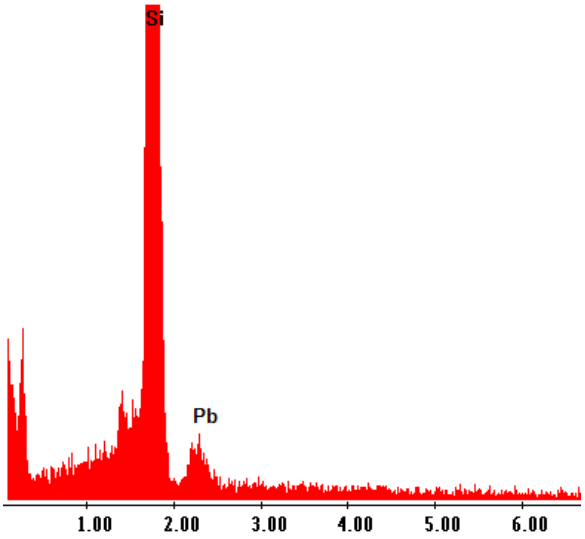

Figure S- 16. SEM-EDX spectrum of [PbHg5_EH].**

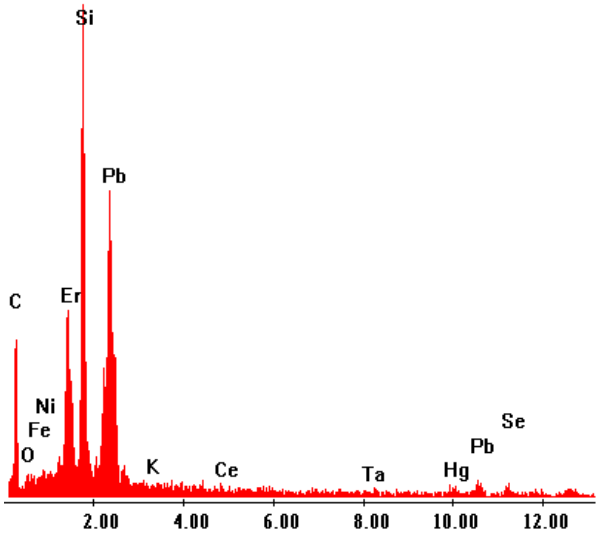

Figure S- 17. SEM-EDX spectrum of [PbHg5.2_2] (1)

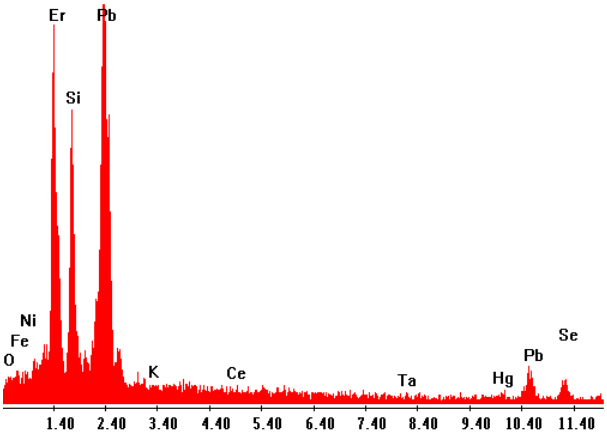

Figure S- 18. SEM-EDX spectrum of [PbHg5.2_2] (2)

**** Note that the peak that is identified as Pb (M-edge) at low x-ray energies corresponds to signal expected from S (K-edge). In fact, when the peak is broad enough, the Hg (M-edge) peak – which lies just a bit lower in energy – will also overlap with the Pb and S peaks[84]. Fortunately, TEM-EDX allows for better detection of higher energy X-rays, enabling unambiguous differentiation between Pb (L-edge) and Hg (L-edge) (and S).**

[84] X-ray absorption edges, for example: http://www.med.harvard.edu/jpnm/physics/refs/xrayemis.html

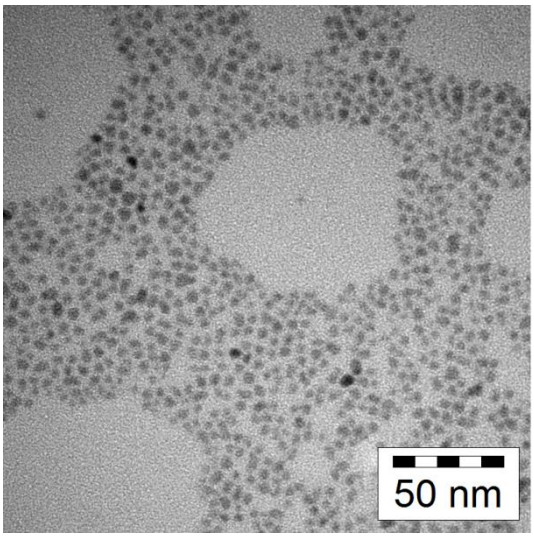

Figure S- 19. TEM-image of PbHg5_EH area on which EDX analysis (1) was performed. Below: Results of the quantification of the EDX-spectrum. It is not know why such a high % of Se is measured (present)

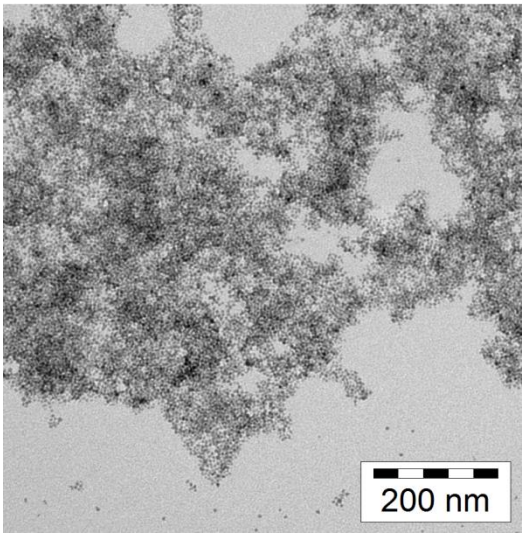

Figure S- 20. TEM-image of PbHg5_EH area on which EDX analysis (2) was performed. Below: Results of the quantification of the EDX-spectrum.

Element	Atomic (%)	Uncertainty (%)	Element	Atomic (%)	Uncertainty (%)
Se (K)	55.158	1.255	Se (K)	48.942	0.425
Hg (L)	35.784	2.037	Hg (L)	13.180	0.522
Pb (L)	13.993	1.305	Pb (L)	37.877	0.897

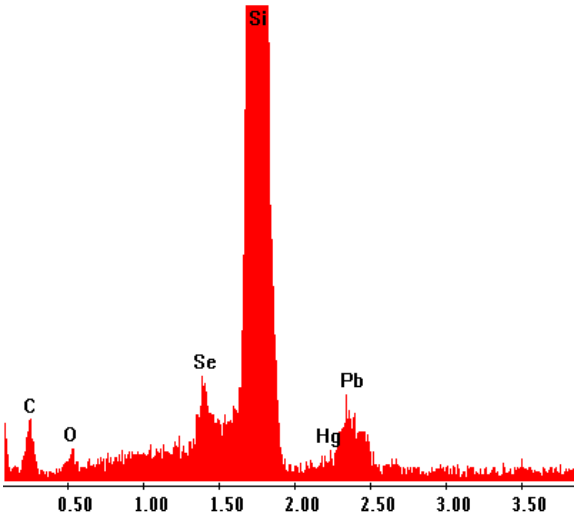

Figure S- 21. SEM-EDX spectrum (1) of super-lattice after addition of Hg(OLAC)2

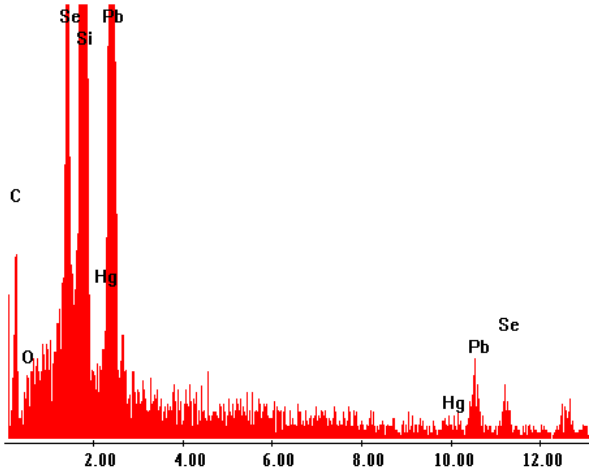

Figure S- 22. SEM-EDX spectrum (2) of super-lattice after addition of Hg(OLAC)2

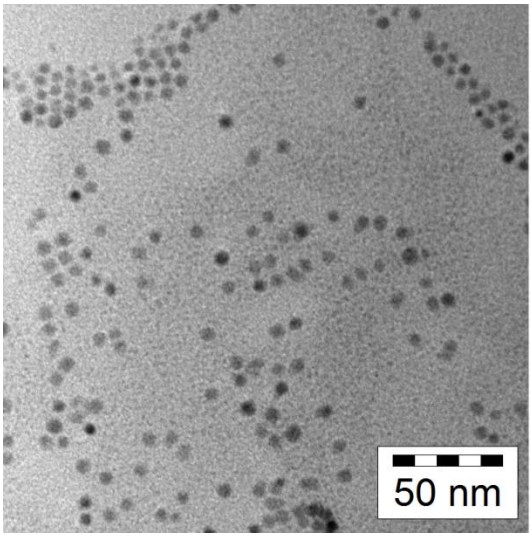

Figure S- 23. TEM image of PbHg5.3_C1

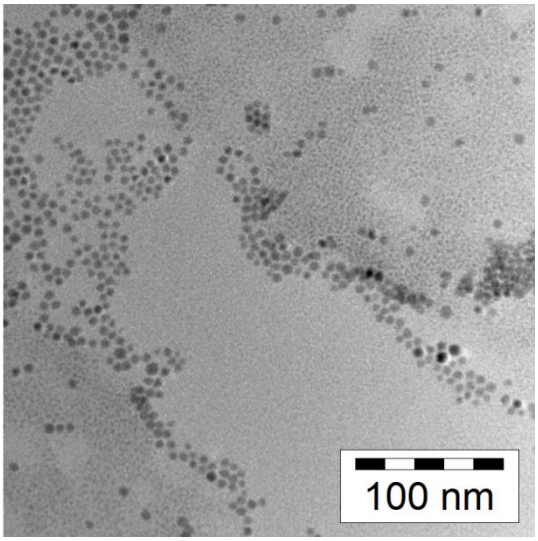

Figure S- 24. TEM image of PgHg5.3_C2

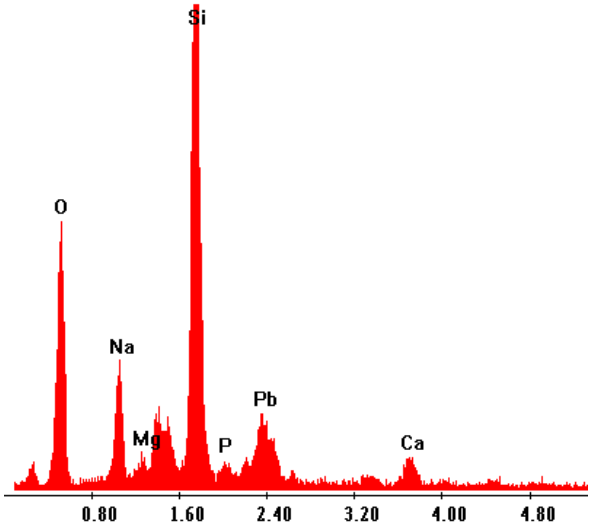

Figure S- 25. SEM-EDX spectrum of PbHg5.3_C2

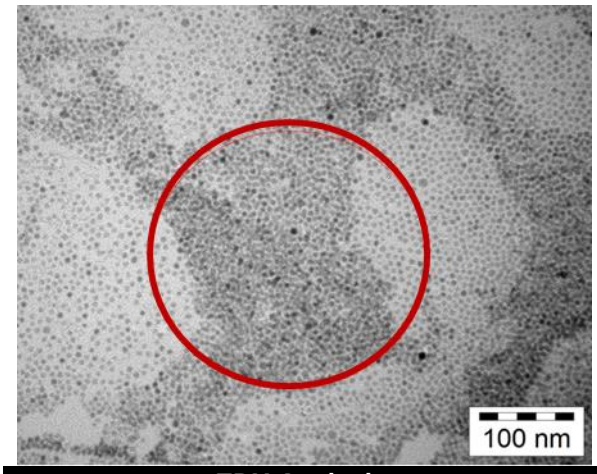

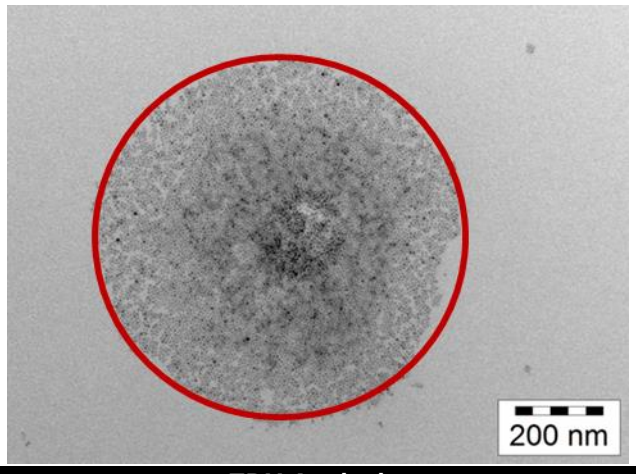

EDX Analysis			EDX Analysis		
Element	**Atomic %**	**Uncertainty %**	**Element**	**Atomic %**	**Uncertainty %**
Se (K)	44.188	0.646	Se (K)	44.188	0.646
Hg (L)	4.316	0.431	Hg (L)	2.39	0.34
Pb (L)	57.417	1.263	Pb (L)	53.42	1.575

Figure S- 26. TEM-EDX analysis of [PbHg8.2_6]

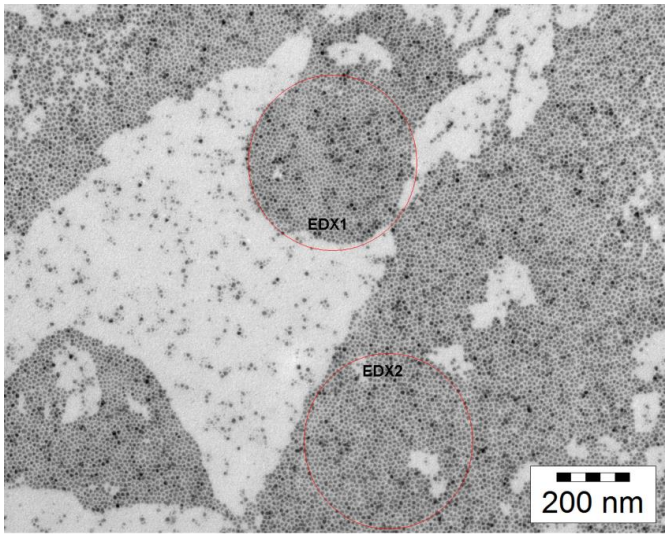

EDX1		
Element	Atomic (%)	Uncertainty (%)
Se (K)	49.224	0.851
Hg (L)	42.384	1.742
Pb (L)	8.390	0.566

EDX2		
Element	Atomic (%)	Uncertainty (%)
Se (K)	45.396	0.506
Hg (L)	52.484	1.024
Pb (L)	2.118	0.292

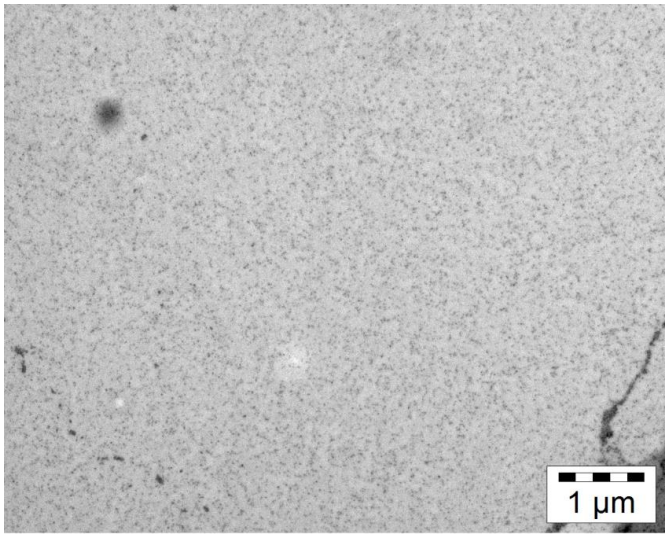

Element	Atomic (%)	Uncertainty (%)
Se (K)	54.085	1.964
Hg (L)	41.145	3.284
Pb (L)	4.769	1.850

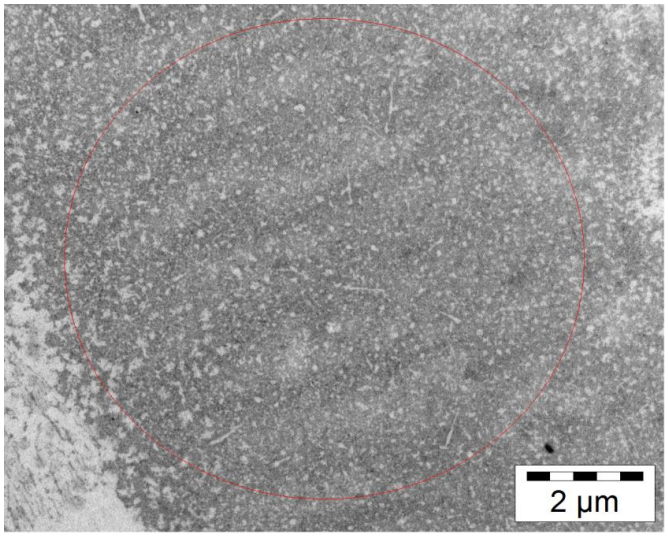

Element	Atomic (%)	Uncertainty (%)
Se (K)	47.387	0.571
Hg (L)	50.478	1.176
Pb (L)	2.143	0.401

Figure S- 27. [PbHg9.2_80-30] TEM-EDX results

Appendix B: Supplementary Tables

Table S- 1. Overview of [PbHg2S] reactions

Name	t	PbSe batch	Precursor	Size (nm)	Shape
PbHg2S_1	30	PbSe 3.3 nm	[PreHgS2]	3.2 +/- 0.5	Spherical
PbHg2S_2	30	PbSe 3.3 nm	[PreHgS2] + C_8NH	3.2 +/- 0.3	Spherical
PbHg2S_4	30	PbSe 3.3 nm	[PreHgS1]	3.1 +/- 0.4	Spherical

Table S- 2. Overview of [PbHg3S] reactions

Name	t	PbSe batch	Precursor	Size (nm)	Shape
PbHg3S_1	30	PbSe 5 nm #1	[PreHgS1]	4.0 +/- 0.3	Spherical
PbHg3S_3	0.5	PbSe 5 nm #1	[PreHgS1]	3.9 +/- 0.5	Spherical

Table S- 3. Overview of [PbHg3.3] reactions

Name	Time (min)	Size (nm)	Shape	Heating T (°C), t (min)	Short description
PbHg3.3_A	1	Too aggregated to measure	Spherical	70, 15	Aggregates, etched
PbHg3.3_B	1	Too aggregated to measure	Spherical	70, 30	Aggregates,
PbHg3.3_C	1	3.9 +/- 0.5	Spherical	50, 15	Partially attached, aggregates in mixture
PbHg3.3_D	1	3.4 +/- 0.5	Spherical	50, 30	Partially attached, aggregates in mixture
PbHg3.3_E	30	3.9 +/- 0.4	Spherical	50, 15	Partially attached, aggregates in mixture
PbHg3.3_F	30	3.7 +/- 0.5	Spherical	50, 60	Partially attached, aggregates in mixture
PbHg3.3_G	30	4.0 +/- 0.4	Spherical	OA + 50, 15	Partially attached, aggregates in mixture
PbHg3.3_H	30	3.6 +/- 0.4	Spherical	OA + 50, 60	Partially attached, aggregates in mixture
PbHg3.3_ EH-control	1	3.9 +/- 0.5	Spherical, anisotropic, rounded	-	Partially attached
PbHg3.3_ IL-control		6.6 +/- 0.7	Spherical	50, 60	Ripening
PbHg3.3_I	1	3.6 +/- 0.5	Spherical	50, 15	Partially attached, aggregates in mixture
PbHg3.3_J	1	3.9 +/- 0.4	Spherical, anisotropic, rounded	50, 60	Partially attached, aggregates in mixture
PbHg3.3_K	1	3.9 +/- 0.4	Spherical	OA + 50, 15	Partially attached, aggregates, "blurry" TEM-image (due to OLAC)
PbHg3.3_L	1	3.7 +/- 0.4	Spherical	OA + 50, 60	Partially attached, aggregates in mixture
PbHg3.3_M	1	3.7 +/- 0.4	Spherical, anisotropic, rounded	Raw + 45, 15	Partial attached, spherical, very "blurry" TEM-image

PbHg3.3_N	1	3.8 +/- 0.5	Anisotropic, rounded	Raw + 45, 60	Partial attached, spherical
PbHg3.3_O	1	3.7 +/- 0.5	Anisotropic, rounded	Quench + 45, 15	No attachement, polydisperse
PbHg3.3_P	1	-	Anisotropic, rounded	Quench + 45, 60	Formation of large 3D "structures" 50 +/- 10 nm connected by a network of aggregated particles, annealed/attached

Table S- 4. Overview of [PbHg7] reactions

Name	T (°C)	Time (min)	(Hg:Pb)	Size (nm)	Shape	Antisolvents (vol. eq. to vol. reaction mix.), time of solvent evaporation at 80 °C
PbHg7_A	RT	0.5	1	3.7 +/- 0.7	Anisotropic	1 BuOH, 1 MeOH, 20
PbHg7_A2	RT	0.5	1	3.4 +/- 1.0	Anisotropic	1 BuOH, 1 MeOH, 40
PbHg7_B	RT	0.5	1	3.9 +/- 0.6	Anisotropic	1 BuOH, 2 MeOH, 20
PbHg7_B2	RT	0.5	1	5.0 +/- 1.0 3.2 +/- 0.5	Anisotropic	1 BuOH, 2 MeOH, 40
PbHg7_C	RT	0.5	1	4.0 +/- 1.3	Anisotropic	1 BuOH, 1 MeOH, PEG, 20
PbHg7_D*	RT	0.5	1	5.0 +/- 0.8 1.8 +/- 0.3	Anisotropic	1 BuOH, 1 MeOH, 20
PbHg7_E	RT	0.5	1	3.9 +/- 0.5	Spherical	Thiol
PbHg7.2_1	RT	0.5	1	3.9 +/- 0.8	Anisotropic	1 BuOH, 3 MeOH, 50
PbHg7.2_2	RT	0.5	1	3.2 +/- 0.4	Anisotropic	1 BuOH, 3 MeOH, 50

**** With Excess OLAM***

Table S- 5. Overview of [PbHg4N] reactions

Name	Time (min)	Precursor	(Pb:Hg) ratio	Size (nm)	Shape	Short description
PbHg4N_A	0.5	PreHg_2	(2:1)	3.2 +/- 0.6	Anisotropic	Polydisperse, aggregates in mixture
PbHg4N_B	0.5	PreHg_2 +OLAM	(2:1)	3.6 +/- 0.5	Anisotropic, rounded	Aggregates in mixture
PbHg4N_C	30	PreHg_2	(2:1)	3.5 +/- 0.4	Anisotropic, rounded	Partial attachment? Aggregates in mixture
PbHg4N_D	30	PreHg_2 +OLAM	(2:1)	3.4 +/- 0.4	Spherical	Partial attachment? Aggregates in mixture
PbHg4N_E	0.5	PreHg_2	(1:2)	3.0 +/- 0.4	Anisotropic, rounded, angular	Small particles
PbHg4N_F	0.5	PreHg_2 +OLAM	(1:2)	3.5 +/- 0.5	Anisotropic, rounded, angular	Elongated (elipoidal) particles
PbHg4N_G	30	PreHg_2	(1:2)	3.3 +/- 0.5	Anisotropic, rounded, angular	2 species of particles?
PbHg4N_H	30	PreHg_2 +OLAM	(1:2)	3.7 +/- 0.6	Anisotropic, angular	Polydisperse
PbHg4N_I	0.5	PreHg_2	(1:1)	3.6 +/- 0.4	Anisotropic, angular	
PbHg4N_J	0.5	PreHg_2 +OLAM	(1:1)	3.7 +/- 0.4	Spherical	Partial attachment? Blurry (dirty) TEM-photo
PbHg4N_K	0.5	PreHg_2	(5:4)	3.6 +/- 0.5	Anisotropic	Blurry (dirty) TEM-photo
PbHg4N_L	0.5	PreHg_2 +OLAM	(5:4)	3.4 +/- 0.5	Spherical, anisotropic, rounded	Partial attachment? Blurry (dirty) TEM-photo

PbHg4N_M	30	PreHg_2	(1:1)	3.9 +/- 0.5	Anisotropic, rounded, angular	
PbHg4N_N	30	PreHg_2 +OLAM	(1:1)	3.9 +/- 0.4	Anisotropic, rounded	
PbHg4N_O	30	PreHg_2	(5:4)	3.6 +/- 0.6	Spherical	Polydisperse
PbHg4N_P	30	PreHg_2 +OLAM	(5:4)	3.6 +/- 0.5	Spherical	Blurry (dirty) TEM-photo

Table S- 6. Overview of [PbHg5] reactions

Name	T	t (min)	(Pb:Hg) ratio	Size (nm)	Shape	Short decription
PbHg5_A-test	RT	0.5	1:1	3.1 +/- 0.4	Spherical	Only found few very small particles and assembly of PbSe particles
PbHg5_A	RT	0.25	1:1	4.0 +/- 1.1	Anisotropic	Many different species, ordered, but also very polydisperse particles present
PbHg5_B	RT	0.75	1:1	10 - 3	Anisotropic	All different types and sizes present
PbHg5_C	RT	2	1:5	4.6 +/- 1.1	Anisotropic	All different types and sizes present
PbHg5_D	RT	5	1:13.2	3.9 +/- 1.3	Anisotropic	Larger and smaller particles, round but also very anisotropic
PbHg5_A-D	RT	5	1:13.2	small and large ~ 7	Anisotropic and spherical	Large spheres and small anisotropic particles, blurry (dirty) TEM-photo, hard to measure
PbHg5_E-test	50	0.5	1:1	3.7 +/- 0.7	Anisotropic	Quite blurry (dirty) TEM-photo
PbHg5_E	50	0.25	1:1	4.2 +/- 0.8	Anisotropic	
PbHg5_F	50	0.75	1:1	3.4 +/- 0.7	Anisotropic	
PbHg5_G	50	2	1:5	3.9 +/- 0.7	Anisotropic	
PbHg5_H	50	5	1:13.2	4.0 +/- 0.6	Anisotropic	Partially attached; some fusion of smaller particles into larger anisotropic ones
PbHg5_E-H	50	5	1:13.2	3.5 +/- 0.4	Spherical	Quite nice, shape and size roughly retained, albeit smaller particles
PbHg5_I-test	100	0.5	1:1	8.4, 2.7**	-	Aggregates, 2 particles measured
PbHg5_I	100	0.25	1:1	-	-	Aggregates, different particles present small, large, near original
PbHg5_J	100	0.75	1:1	-	-	Aggregates
PbHg5_K	100	2	1:5	-	-	Aggregates
PbHg5_L	100	5	1:13.2	-	-	Aggregates
PbHg5_I-L	100	5	1:13.2	3.9 +/- 0.8	Anisotropic	Lots of aggregates, small colony of particles found and measured

Table S- 7. Overview of [PbHg5.2_X] and [PbHg5.3_X] reactions

Name	T (°C)	t (min)	(Pb:Hg)	Size (nm)	Shape	Work up	Short description
PbHg5.2_1	RT	0.5	(1:1)	4.3 +/- 0.6	Spherical,	-	Attachment
PbHg5.2_2	RT	0.5	(1:13.2)	3.5 +/- 0.6 2.7 +/- 0.5	Anisotropic	-	Different species present
PbHg5.2_3	50	0.5	(1:1)	4.3 +/- 0.5	Anisotropic,	-	Attachment
PbHg5.2_4	50	0.5	(1:13.2)	1.8 +/- 0.1 3.1 +/- 0.5	Anisotropic,	-	Accuracy on small particles

							questionable - limite of TEM resolution, attachment
PbHg5.2_5	RT	0.5	(1:1)	2.7 +/- 0.6**	Anisotropic,	ODT+TOP, 30 min, T=50	Huge aggregates + small attached anisotropic
PbHg5.2_6	RT	0.5	(1:13.2)	2.9 +/- 0.5	Spherical	ODT+TOP, 30 min, T=50	
PbHg5.3_A1	RT	30	(1:13.2)	3.4 +/- 0.9	Anisotropic		Attachment
PbHg5.3_A2	RT	30	(1:13.2)	~ 3.3	Anisotropic	ODT+TOP, 30 min, T=50	Blurry (dirty) TEM photo
PbHg5.3_B1	RT	30	(1:13.2)	4.3 +/- 0.5	Spherical		Aggregates present
PbHg5.3_B2	RT	30	(1:13.2)	4.7 +/- 1.1 ~ 1.2	Anisotropic	ODT+TOP, 30 min, T=50	Large and very small particles
PbHg5.3_C1 + 30 µL ODT v/s 2.40 mL $Hg(OLAC)_2$	50	30	(1:13.2)	4.7 +/- 1.0	Spherical	ODT	Very small particles present
PbHg5.3_C2 + 30 µL ODT v/s 2.40 mL $Hg(OLAC)_2$	50	30	(1:13.2)	5.1 +/- 0.9	Spherical	DDT	Very small particles present. Aggregates formed

Table S- 8. Overview of [PbHg6] and [PbHg8, 8.2]

Name	T (°C)	t (min)	Solvent	Hg-precursor	(Hg:Pb)	Size (nm)	Shape	Short description
PbHg6_3	50	30	Tol	[PreHg5.2]	~100	3.6 +/- 1.6	Spherical	Many different sizes present
PbHg6_4	50	30	Tol	[PreHg5.3]	~10	-	-	Blurry (dirty) TEM image
PbHg6_2	50	30	Tol	[PreHg5.3]	~10	~ 4.5	Anisotropic	Blurry (dirty) TEM image
PbHg8_5	80	0,5	Tol	[PreHg4]	1	4.7 +/- 0.5	Spherical	
PbHg8_6	80	0,5	OLAM	[PreHg4]	1	4.1 +/- 0.9	Spherical	
PbHg8.2_2	RT	0,5	OLAM	[PreHg4]	1	5.1 +/- 0.6 ~ 1.2	Spherical	
PbHg8.2_4	50	0,5	OLAM	[PreHg4]	1	4.9 +/- 0.6	Spherical	
PbHg8.2_6	80	0,5	OLAM	[PreHg4]	1	5.0 +/- 0.9	Spherical	

Appendix C: List of figures

Figure 1. The striking example of quantum confinement in CdSe quantum dots. Figure taken from [1]. 4

Figure 2. TEM-images of PbSe NCs. Top left: [PbSe 3.3 nm]. Top right: [PbSe 5 nm #1]. Bottom left: [PbSe 5 nm #2]. Bottom right: [PbSe 5 nm #3]. 11

Figure 3. Reaction mechanism of $Hg(OLAC)_2$ formation. R = $-(CH_2)_7HC=CH(CH_2)_7CH_3$. ODE is used as solvent. 13

Figure 4. Results of pilot experiments. A;B;C) TEM images of [PbHg1_1], [PbHg1_3], [PbHg1_4] resp.; D;E) HAADF-STEM images of [PbHg1_3]; F) EDX-spectrum of [PbHg1_3]. 15

Figure 5. TEM images of A) (2D)-triangular NCs, (actual sample: [PbHg3_4]); B) Anisotropic NCs (actual sample [PbHg4_1]). 17

Figure 6. TEM-image of a typical [PbHg3.3], [PbHg4N] or [PbHg7, 7.2] result (original sample: [PbHg4N_G]). 18

Figure 7. TEM-images of the temporal evolution of NCs in solution: A) [PbHg5_A]; B) [PbHg5_B]; C) [PbHg5_E]; D) [PbHg5_F]; E) [PbHg5_EH]; F) [PbSe 5 nm #1] 20

Figure 8. TEM-images of PbSe NCs super-lattices. Left, before addition of Hg-precursor – average diameter 3.5 +/- 0.2 nm; right, after Hg-precursor addition – average diameter 2.7 +/- 0.3 nm. 22

Figure 9. TEM-images of [PbHg9], the image labels correspond to X = A,B,C, respectively 25

Figure 10. TEM-images of temporal evolution of [PbHg9.2]. Left column represents a 50 °C series, the right column represents 80 °C. Labels correspond to the time in minutes. 27

Figure 11. TEM-images of [PbHg9.3], the image labels correspond to X = A,B,C,D respectively 29

Figure 12. TEM images of [PbHg13]. The left collumn shows results of experiments performed at 80 C, the right represents experiments performed at 120 °C. The label corresponds to the ligand mixture used in the ligand exchange step. 31

Figure 13. EDX-analysis of [PbHg13_TOP2] 32
Figure 14. EDX analysis of [PbHg13_ODE, ODE2] 32
Figure 15. EDX analysis of [PbHg13_Pyr, Pyr2] 33
Figure 16. Absorption spectrum of [PbHg13_Pyr2]. 34
Figure 17. Schematic representation of HgSe formation 37

Figure 18. TEM-images of HgSe NCs prepared by Howes et al. through different synthesis methods. Scale bars represent 50 nm. 39

Figure 19. a) TEM-image of HgTe NCs obtained by Keuleyan et al.; b) HR-TEM images of the same crystals. 39

Figure S- 1. Optical measurements of [PbSe 3.3 nm] 44
Figure S- 2. Optical measurements of [PbSe 5 nm #1] 44
Figure S- 3. Absorption spectrum of [PbSe 5 nm #2] 44
Figure S- 4. Absorption spectrum of [PbSe 5 nm #3] 44
Figure S- 5. EDX-analysis of [PbSe 5 nm #1] 45
Figure S- 6. Absorption spectra of pilot experiments 46
Figure S- 7. Emssion spectra of pilot experiments 46
Figure S- 8. TEM-image of [PbHg2_-10] 46
Figure S- 9. TEM-image of [PbHg2_RT] 46
Figure S- 10. TEM image of [PbHg2S_4] 47
Figure S- 11. TEM image of PbHg3S_1 47
Figure S- 12. TEM-EDX spectrum (1) of PbHg3S_1 47
Figure S- 13. HAADF image corresponding to TEM-EDX(1) of PbHg3S_1 47
Figure S- 14. TEM-EDX spectrum (2) of PbHg3S_1 47
Figure S- 15. HAADF image corresponding to TEM-EDX(2) of PbHgS3_1 47
Figure S- 16. SEM-EDX spectrum of [PbHg5_EH].** 48
Figure S- 17. SEM-EDX spectrum of [PbHg5.2_2] (1) 48
Figure S- 18. SEM-EDX spectrum of [PbHg5.2_2] (2) 48

Figure S- 19. TEM-image of PbHg5_EH area on which EDX analysis (1) was performed. Below: Results of the quantification of the EDX-spectrum. It is not know why such a high % of Se is measured (present) 49

Figure S- 20. TEM-image of PbHg5_EH area on which EDX analysis (2) was performed. Below: Results of the quantification of the EDX-spectrum. 49

Figure S- 21. SEM-EDX spectrum (1) of super-lattice after addition of Hg(OLAC)2 49
Figure S- 22. SEM-EDX spectrum (2) of super-lattice after addition of Hg(OLAC)2 49
Figure S- 23. TEM image of PbHg5.3_C1 50
Figure S- 24. TEM image of PgHg5.3_C2 50
Figure S- 25. SEM-EDX spectrum of PbHg5.3_C2 50
Figure S- 26. TEM-EDX analysis of [PbHg8.2_6] 51
Figure S- 27. [PbHg9.2_80-30] TEM-EDX results 52

Figure S- 28. CdSe-synthesis results: A) TEM micrograph; B) XRD diffractogram; C) Absorption spectrum 61

Appendix D: List of Tables

Table 1. List of Chemicals 8
Table 2. PbSe Nanocrystal Properties 11
Table 3. $Hg(OLAC)_2$ precursors 13
Table 4. Experimental conditions and results of pilot experiments 14
Table 5. Experimental conditions and results for [PbHg2_RT] & [PbHg2_-10] 16
Table 6. [PbHg3], [PbHg3.2] conditions and results 17
Table 7. Results and conditions of first samples taken from [PbHg5] 18
Table 8. Conditions and results of [PbHg9] 25
Table 9. Results and conditions of [PbHg9.2] 26
Table 10. Results and conditions of [PbHg9.3] 28
Table 11. Ligand exchange conditions for [PbHg13L]. All quantities are in mL. 30
Table 12. Results and conditions of [PbHg13]. 30
Table 13. Relative crystal component ratio's 36

Table S- 1. Overview of [PbHg2S] reactions 53
Table S- 2. Overview of [PbHg3S] reactions 53
Table S- 3. Overview of [PbHg3.3] reactions 53
Table S- 4. Overview of [PbHg7] reactions 54
Table S- 5. Overview of [PbHg4N] reactions 54
Table S- 6. Overview of [PbHg5] reactions 55
Table S- 7. Overview of [PbHg5.2_X] and [PbHg5.3_X] reactions 55
Table S- 8. Overview of [PbHg6] and [PbHg8, 8.2] 56

Appendix F: Synthesis of CdSe and subsequent cation exchange to Cu_2Se

As alternative starting point for cation exchange (being CdSe -> CuSe -> HgSe), CdSe NCs with the cubic zinc blende were synthesized. For this synthesis the procedure by Li et al.[85] was used. The reaction was carried out in the schlenkline under N_2. Stepwise a typical synthesis can be described as follows:

1. $Cd(OLAC)_2$ precursor preparation

$0.40*10^{-3}$ mol $CdAc_2$ was dissolved in $1.0*10^{-3}$ mol OLAC and 3 mL ODE in a 50 mL three-neck roundbottom flask by heating the mixture to 120 °C under N_2 flow, yielding a *colorless solution*. After dissolution the mixture was degased under vacuum at 100 °C for 1 hour and left to cool to RT.

2. CdSe formation: heating up

The cooled mixture was added to a 50 mL three-neck roundbottom flask containing $0.30*10^{-3}$ mol *black* selenium powder. Subsequently, the temperature was increased to 240 °C. *At 180 °C the selenium powder dissolved. At 200 °C the solution turned orange.* After maintaining a temperature of ~ 240 °C for 5 minutes the solution was cooled to RT. After cooling *the mixture has a red color*.

3. Purification

The CdSe NPs were precipitated by adding a mixture of BuOH/MeOH (3:1). After centrifugation they were dispersed in toluene and subjected to two more washing cycles using MeOH and toluene. After synthesis the particles were analyzed using TEM, PLS and XRD.

The results of the CdSe synthesis are shown in figure S28. An example TEM-figure is shown. Average particle diamter was determined to be 3.61 +/- 0.39 nm. The zinc blende structure of the NCs was determined from comparison to known ZB CdSe QDs[86]. The sharp peaks originate from the Si-substrate.

Cation exchange was carried out according to an adapter procedure from the same work as the ZB CdSe synthesis by Li et al.. First, CdSe was diluted in toluene to having a cation concentration of $5{,}50*10^{-3}$ mol Cd^{2+} / mL. To this solution 15 µL TOP was added. Second, $0.04*10^{-3}$ mol tetrakis in 2 mL MeOH was added *resulting in a color change from red to black*. Finally the Cu_2Se NCs were pelleted and washed two times with MeOH/Tol.

Further analysis was not performed.

Cu_2Se has successfully been used in sequential CE. It's monovalency provides a driving force that is exploited in transformations, where a direct exchange is unsuccessfull[87]. As such the formation of an intermediate ZB Cu_2Se could be used en route to the formation of HgSe NCs.

If anyone would take up such a route and encounter irreversible aggregation during CE, he or she should screen different ligand additions (type & concentration) to the pre-CE NC containing mixture. In the case presented above, the addition of a small amount of TOP resulted in a successful exchange, whereas it was not mentioned in the reference paper used.

[85] Li et al., Nano lett. 2011, 11, 4964

[86] Mohamed et al., J. Phys. Chem. B 2005, 109 (21), 10533-10537; Also, the XRD-pattern of a "failed" CdSe synthesis, where bulk material was formed, showed a different XRD-pattern; CdSe has a hexagonal wurtzite structure in the bulk.

[87] Rivest et al., Chem. Soc. Rev. 2013, 42(1), 89

* If the initial TOP-less synthesis results in aggregate formation, it is recommended to perform a series of experiments in the presence of different amounts of additional ligands. Here, no TOP causes aggregation, whereas too much TOP prevents the exchange.

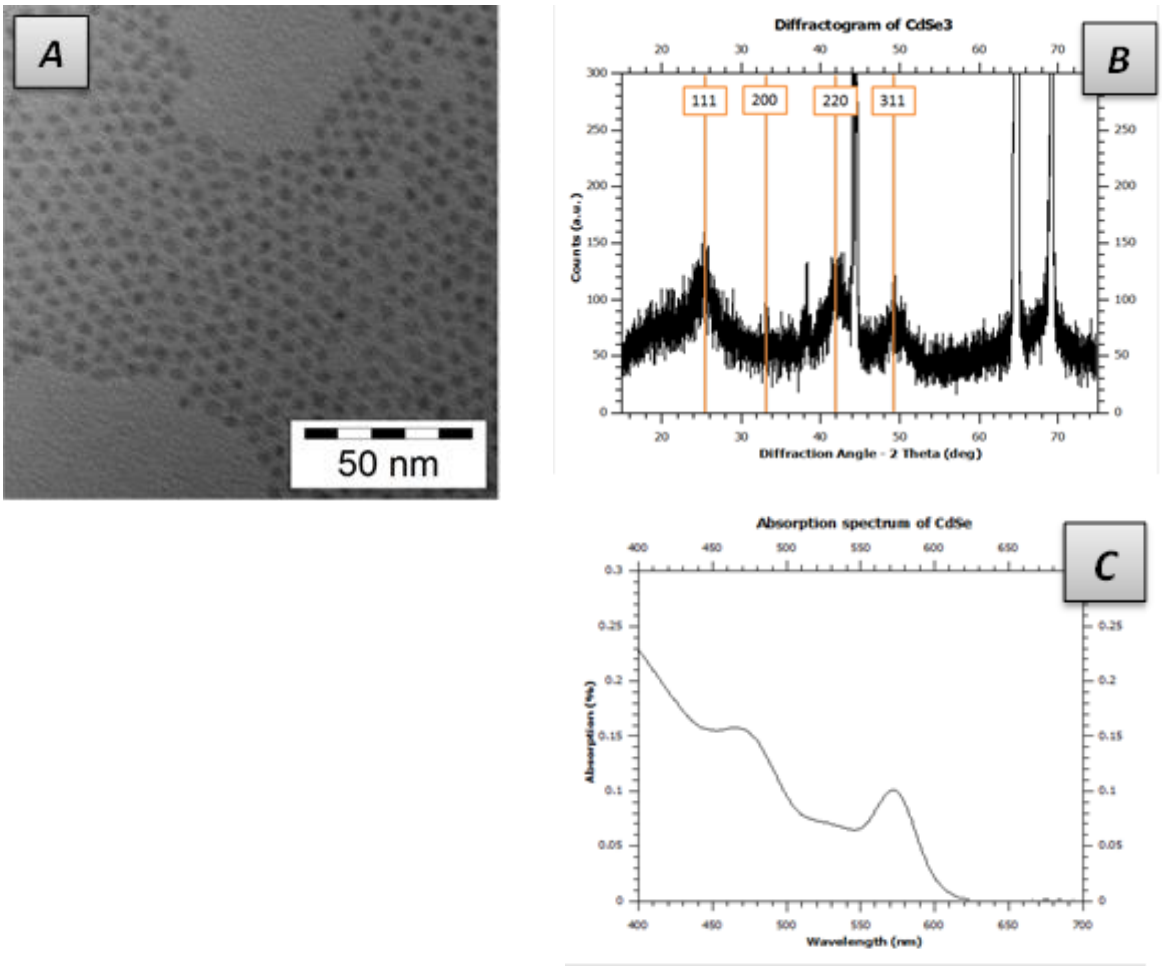

Figure S- 28. CdSe-synthesis results: A) TEM micrograph; B) XRD diffractogram; C) Absorption spectrum